Universidade de Aveiro Departamento de
2011 Electrónica, Telecomunicações e Informática

**Paulo Dionísio
Reinas Serralheiro**

**Implementação de um Sistema de Comunicações
Móveis para o Uplink**

**Paulo Dionísio
Reinas Serralheiro**

**Implementação de um Sistema de Comunicações
Móveis para o Uplink**

o júri / the jury

presidente / president

Prof. Dr. José Carlos da Silva Neves

Professor Catedrático do Departamento de Electrónica, Telecomunicações e Informática da Universidade de Aveiro

orientador / adviser

Prof. Dr. Adão Paulo Soares da Silva

Professor Auxiliar do Departamento de Electrónica, Telecomunicações e Informática da Universidade de Aveiro

co-orientador / co-adviser

Prof. Dr. Atílio Manuel da Silva Gameiro

Professor Associado do Departamento de Electrónica, Telecomunicações e Informática da Universidade de Aveiro

arguente / examiner

Prof. Dr. Paulo Jorge Coelho Marques

Professor Adjunto do Instituto Politécnico da Escola Superior de Tecnologia de Castelo Branco

resumo   É evidente que actualmente cada vez mais a internet móvel está presente na vida das sociedades. Hoje em dia é relativamente fácil estar ligado à internet sempre que se quiser, independentemente do lugar onde se encontra (conceito: anytime and anywhere). Desta forma existe um número crescente de utilizadores que acedem a serviços e aplicações interactivas a partir dos seus terminais móveis. Há, portanto, uma necessidade de adaptar o mundo das telecomunicações a esta nova realidade, para isso é necessário implementar novas arquitecturas que sejam capazes de fornecer maior largura de banda e reduzir os atrasos das comunicações, maximizando a utilização dos recursos disponíveis do meio/rede e melhorando assim a experiência do utilizador final.

O LTE representa uma das tecnologias mais avançadas e de maior relevância para o acesso sem fios em banda larga de redes celulares. OFDM é a tecnologia base que está por traz da técnica de modulação, bem como as tecnologias adjacentes, OFDMA e SC-FDMA, usadas especificamente no LTE para a comunicação de dados descendente (downlink) ou ascendente (uplink), respectivamente. A implementação de múltiplas antenas em ambos os terminais, potenciam ainda mais o aumento da eficiência espectral do meio rádio permitindo atingir grandes taxas de transmissão de dados.

Nesta dissertação é feito o estudo, implementação e avaliação do desempenho da camada física (camada 1 do modelo OSI) do LTE, no entanto o foco será a comunicação de dados ascendente e a respectiva técnica de modelação, SC-FDMA. Foi implementada uma plataforma de simulação baseada nas especificações do LTE UL onde foram considerandos diferentes esquemas de antenas. Particularmente para o esquema MIMO, usou-se a técnica de codificação no espaço-frequência proposta por Alamouti. Foram também implementados vários equalizadores.

Os resultados provenientes da simulação demonstram tanto a eficiência dos diversos modos de operação em termos da taxa de erro, como o excelente funcionamento de processos de mapeamento e equalização, que visam melhorar a taxa de recepção de dados.

keywords

abstract

It is clear that mobile Internet is present in the life of societies. Nowadays it is relatively easy to be connected to the internet whenever you want, no matter where you are (concept: anytime and anywhere). Thus, there are a growing number of users accessing interactive services and applications from their handsets. Therefore, there is a need to adapt the world of telecommunications to this new reality, for that it is necessary to implement new architectures that are able to provide higher bandwidth and reduce communication delays, maximizing use of available resources in the medium/network and thereby improving end-user experience.

LTE represents one of the most advanced architectures and most relevant to wireless broadband cellular networks. OFDM is the technology that is behind the modulation technique and the underlying technologies, OFDMA and SC-FDMA, used specifically in LTE for data communication downward (downlink) or upward (uplink), respectively. The implementation of multiple antennas at both ends further potentiate the increase of spectral efficiency allowing to achieve high rates of data transmission.

In this dissertation is done the study, implementation and performance evaluation of the physical layer (OSI Layer 1) of the LTE, but the focus will be communication and its upstream data modeling technique, SC-FDMA. We implemented a simulation platform based on LTE UL specifications where were considered different antenna schemes. Particularly for the MIMO scheme, we used the technique of space-frequency coding proposed by Alamouti. We also implemented several equalizers.

The results from the simulation demonstrate both the efficiency of different modes of operation in terms of error rate, as the excellent operation of mapping processes and equalization, designed to improve the rate of receiving data.

Contents

List of Figures

List of Tables

Acronyms

1×EV-DO	One Carrier Evolved, Data Optimized
1×EV-DV	One Carrier Evolved, Data Voice
1×RTT	One Carrier Radio Transmission Technology
16-QAM	16 Quadrature Amplitude Modulation
1G	First Generation
2G	Second Generation
3G	Third Generation
3GPP	Third Generation Partnership Project
3GPP2	Third Generation Partnership Project 2
4G	Fourth Generation
64-QAM	64 Quadrature Amplitude Modulation
8-PSK	Octagonal Phase Shift Keying
AGW	Access Gateway
ARQ	Automatic Repeat Request
BER	Bit Error Rate
bps	bits per second
BPSK	Binary Phase Shift Keying
CAPEX	Capital Expenditure
CAZAC	Constant Amplitude Zero Autocorrelation
CDMA	Code Division Multiple Access
CDMA2000	Code Division Multiple Access 2000
CP	Cycle Prefix
dB	Decibel
DL	Downlink
EDGE	Enhanced Data rates for GSM Evolution
eNodeB	Evolved Node B
EPC	Evolved Packet Core
EPC	Evolved Packet Core
EPS	Evolved Packet System
EPS	Evolved Packet System
E-RAN	Evolved Radio Access Network
E-UTRA	Evolved UMTS Terrestrial Radio Access
E-UTRAN	Evolved UMTS Terrestrial Radio Access Network
EV-DO	One Carrier Evolved, Data Optimized
EV-DV	One Carrier Evolved, Data Voice
FDD	Frequency Division Duplex

FDM	Frequency Division Multiplexing
FFT	Fast Fourier Transform
GERAN	GSM EDGE Radio Access Network
GGSN	Gateway GPRS Support Node
GMSK	Gaussian Minimum Shift Keying
GPRS	General Packet Radio Service
GSM	Global System for Mobile
HLR	Home Location Register
HRPD	High Rate Packet Data
HRPD	High Rate Peak Data
HSDPA	High Speed Downlink Packet Access
HSPA	High Speed Packet Access
HSPA+	HSPA Evolution
HSS	Home Subscriber Server
HSUPA	High Speed Uplink Packet Access
Hz	Hertz
ICI	Inter-Carrier Interference
ICIC	Inter-Cell Interference Coordination
IFFT	Inverse Fast Fourier Transform
IMS	IP Multimedia Subsystem
IMT-2000	International Mobile Telecommunications 2000
IP	Internet Protocol
ISI	Inter-Symbol Interference
IT	Institute of Telecommunications
ITU	International Telecommunications Union
LAN	Local Area Network
LTE	Long Term Evolution
MAN	Metropolitan Area Network
MBMS	Multimedia Broadcast Multicast Service
MIMO	Multiple Input Multiple Output
MISO	Multiple Input Single Output
MME	Mobile Management Entity
OFDM	Orthogonal Frequency Division Multiplexing
OFDMA	Orthogonal Frequency Division Multiple Access
OPEX	Operational Expenditure
OSI	Open Systems Interconnection
PAPR	Peak-to-Average Power Ratio
PAR	Peak-to-Average Ratio
PCRF	Policy Control and Charging Rules Function
PDN-GW	Packet Data Network Gateway

PSTN	Public Switched Telephone Network
QAM	Quadrature Amplitude Modulation
QoS	Quality of Service
QPSK	Quadrature Phase Shift Keying
RAN	Radio Access Network
RNC	Radio Network Controller
RRC	Radio Resource Control
SAE	System Architecture Evolution
SC-FDMA	Single Carrier Frequency Division Multiple Access
SFBC	Space Frequency Block Coding
SGSN	Serving GPRS Support Node
S-GW	Serving Gateway
SIMO	Single Output Multiple Output
SINR	Signal to Interference-plus-Noise Ratio
SISO	Single Output Single Output
SNR	Signal Noise Ratio
STBC	Space Time Block Coding
STC	Space Time Coding
TDD	Time Division Duplex
TTI	Transmission Time Interval
UE	User Equipment
UL	Uplink
UMB	Ultra Mobile Broadband
UMTS	Universal Mobile Telecommunications System
UTRA	Universal Terrestrial Radio Access
UTRAN	Universal Terrestrial Radio Access Network
VoIP	Voice over Internet Protocol
WAN	Wide Area Network
W-CDMA	Wideband Code Division Multiple Access
WIFI	Wireless Fidelity
WIMAX	Worldwide Interoperability for Microwave Access
WLAN	Wireless Local Area Network
WMAN	Wireless Metropolitan Area Network

"I do not think that the wireless waves I have discovered will have any practical application."

Heinrich Rudolf Hertz

Chapter 1

1. Introduction

The Global System for Mobile communications (GSM) is the dominant wireless cellular standard with over 3.5 billion subscribers worldwide covering more than 85% of the global mobile market. Furthermore, the number of worldwide subscribers using High Speed Packet Access (HSPA) networks topped 70 million in 2008 [1]. HSPA is a Third Generation (3G) evolution of GSM supporting high speed data transmissions using Wideband Code Division Multiple Access (W-CDMA) technology. Global uptake of HSPA technology among consumers and businesses is accelerating, indicating continued traffic growth for high speed mobile networks worldwide. In order to meet the continued traffic growth demands, an extensive effort has been underway in the Third Generation Partnership Project (3GPP) to develop a new standard for the evolution of GSM/HSPA technology towards a packet optimized system referred to as Long Term Evolution (LTE).
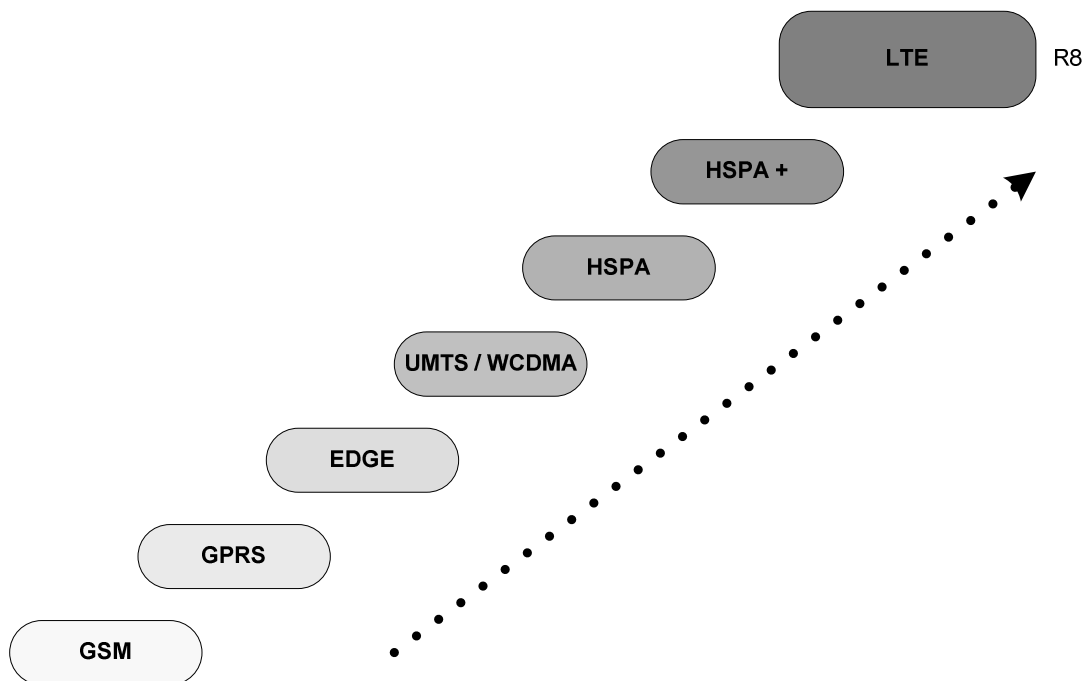
Figure 1 - Mobile Technologies Evolution

The goal of the LTE standard is to create specifications for a new radio access technology geared to higher data rates, low latency and greater spectral efficiency. The spectral efficiency target for

the LTE system is three to four times higher than the current HSPA system or others equivalents. These aggressive spectral efficiency targets require pushing the technology to a new level by employing advanced air interface techniques, such as orthogonal uplink multiple access based on Single Carrier Frequency Division Multiple Access (SC-FDMA) and Multiple Input Multiple Output (MIMO) techniques [1].

From both a technical and practical point of view, there is much to understand, examine and evaluate in the capabilities and benefits that SC-FDMA brings to LTE. SC-FDMA is a hybrid modulation scheme that combines multipath resistance by Orthogonal Frequency Division Multiplexing (OFDM) technology with low peak-to-average power ratio (PAPR) of traditional single-carrier formats, such as GSM, as also presents inter-cell interference mitigation techniques, low-latency channel structure and single frequency network broadcast [2]. Further details concerning these technologies can be found in [3] and [4].

In this thesis we explore what LTE aims to bring to the wireless ecosystem. After considering the broader aspects of LTE, we take a deep look at the uplink, which uses a new modulation format (SC-FDMA). These are interesting times because it is rare that the communications industry rolls out a new modulation format.

1.1. Motivation

The systems of Third Generation are now a reality, having already reached some maturity. This system is based on technology Code Division Multiple Access (CDMA) and uses a band next of 2 GHz, with transmission rates from the 144 kbps for high speed, up to 2 Mbps in inferior environments. The first step in the evolution of this system was given to the implementation of technologies High Speed Downlink Packet Access (HSDPA) for the downward direction (downlink) and High Speed Uplink Packet Access (HSUPA) for the upward direction (uplink). With these technologies it is possible to obtain transmission rates from 1.8 Mbps to about 14.4 Mbps. However, the anticipated increase in demand for broadband services, which require high transmission rates, may not be met in the future with these technologies.

Thus, the Third Generation Partner-Ship Project [5] undertook a research and specification of a new standard, called Long Term Evolution (LTE). This mobile communications system can also be seen as an evolution of current 3G systems, also known as 4G[1], but is based on completely different technology, the Orthogonal Frequency Division Multiple Access (OFDMA) for the downstream (downlink) and Single Carrier Frequency Division Multiple Access (SC-FDMA) for the

---

[1] 4G (Forth Generation) refers the new generation of mobile communications, however taking into account the 3GPP specifications, LTE is considered as 3.9G as described in 3GPP Release 8 and LTE-Advanced is the true matching to 4G as described in 3GPP Release 10, although throughout this thesis we refer to LTE as the Fourth-Generation mobile.

upstream (uplink). One of major objective of this system is to provide future transmission rates of around 100 Mbps for downlink and 50 Mbps for uplink, values well above the current 3G systems.

Portugal Telecom predicts the first commercial systems based on LTE technology, might enter the market in the end of this year. Actually, this process is pending the award of licenses by ANACOM[2].

The analysis of the performance of these systems in settings close to reality requires the use of simulation, so the development of an efficient simulation platform is a tool of extreme importance. The Institute of Telecommunications (IT) already has considerable expertise in this area of research, as part of an active participates in several European projects spearheading the research. The work has been done under the FCT project CADWIN.

1.2. Objectives

The work of this thesis falls under the area of wireless communications and its main goals are study, implement and evaluate the performance of the physical layer of LTE to the uplink.

The aim is to implement a simulation platform based on the LTE UL with multiple MIMO schemes (1×1, 1×2 and 2×2), using the concept of Alamouti for the 2×2 scheme, allowing selection between various equalizers, such as Maximum Ratio Combining (MRC), Equal Gain Combining (EGC), Zero Forcing Combining (ZFC), Minimum Mean Square Error Combining (MMSEC). It is also desirable that allows different modeling schemes (BPSK, QPSK, 16QAM and 64 QAM), variable number of points of FFT modules, adjacent and distributed mapping, as well as allowing multiple users.

After optimizing and validating platform is needed to simulate all scenarios and analyze the results.

---

[2] National Communications Authority in Portugal

1.3. Contributions of this Thesis

The research performed in this work resulted in the following contributions:

- Study of the physical layer specification for the LTE system;

- Integration of a simulation platform for transmitting and receiving data with SC-FDMA modulation, MIMO architecture and consequent performance evaluation;

- Understanding how this communication system improves the efficiency of data reception when used various equalization schemes or other strategies (e.g. the interleaved mode).

1.4. Outline

This thesis is structured as follows. Until the end of this chapter, we made an overview of the technologies used around the world and ended up with the next technology adopted worldwide for cellular network technologies.

In Chapter 2, we first we make a description of the evolution of mobile telecommunication technologies so far, thus, we do a brief introduction over basic concepts of LTE standard and the network architecture that support this technology.

Chapter 3 discusses the main ideas behind the multicarrier techniques that were implemented in this thesis, namely Orthogonal Frequency Division Multiplexing (OFDM) and its multiple access versions, such as Orthogonal Frequency Division Multiple Access (OFDMA), and Single-Carrier Frequency Division Multiple Access (SC-FDMA).

In Chapter 4, we presented the understanding over multi-antenna techniques and emphasizes on mathematical framework for the capacity determination of MIMO systems.

Chapter 5 is the core of this thesis. Here, we present the analysis for physical layer of LTE for the uplink. The model used for computing this wireless communication system is based on SC-FDMA modulation and evaluate simultaneously the performance of the MIMO architecture and the equalizers schemes, as well as the results of the interleaver mode with the ability to simulate multiple users. As also, we provide a more thorough description on the most relevant topic to this work: the mechanisms for equalization support which are specific to that mode.

Finally, in Chapter 6 we conclude this thesis and provide guidelines for future research.

Chapter 2

2. Background

In this chapter we shall introduce the topics, standards and tools which are the groundwork for this thesis. In Section 2.1 we describe in detail the evolution of mobile telecommunication technologies until the present day; In Section 2.2 we introduces the technology of future mobile telecommunication, Long Term Evolution (LTE), and, in particular, its features of operation, upon which we implement and simulate all the work in this thesis; In Section 2.3 we talk about the network architecture, which implements support for LTE; and finally we summarize our research in Section 2.4. At each section also includes references to all of the related work, papers, books and technical reports related to the topics being approached in this thesis.

2.1. Evolution of mobile technologies

The cellular wireless communications industry witnessed tremendous growth in the past decade with over 4 billion wireless subscribers worldwide [1]. The First Generation (1G) analog cellular systems supported voice communication with limited roaming. The Second Generation (2G) digital systems promised higher capacity and consequently better voice quality than did their analog counterparts. Moreover, roaming became more prevalent thanks to fewer standards and common spectrum allocations across countries particularly in Europe. The two widely deployed 2G cellular systems are based in TDMA (Time Division Multiple Access), e.g. GSM (Global System for Mobile Communications) and based in CDMA (Code Division Multiple Access), e.g. IS-95 from cdmaOne. In same way that 1G analog system, 2G systems were primarily designed to support voice communications, however in later releases of these standards, it were introduced capabilities to support data transmission. In this sense new protocols, labeled 2.5G, have emerged, such as GPRS (General Packet Radio Service) for GSM, it could provide data rates of 40 kbps in the downlink and 14 kbps in the uplink by aggregating GSM time slots into one bearer, although enhancements in later releases meant that GPRS could theoretically reach downlink speeds of up to 171 kbps [5], and 1×RTT (One Carrier Radio Transmission Technology) for cdma2000, supporting bi-directional peak data rates up to 153 Kbit/s [6]. To close the 2G, Enhanced Data rates for GSM Evolution (EDGE) is standardized in 2003 by 3GPP as part of the GSM family, also known as Enhanced GPRS (EGPRS), labeled 2.75G. It is an upgrade that provides a potential three-fold increase in capacity of GSM/GPRS networks. The GSM EDGE Radio Access Network (GERAN) group of 3GPP specifies achieve data rates up to 384 Kbit/s by switching to more sophisticated methods of coding (8PSK replacing GMSK) within existing GSM timeslots.

Ongoing standards work in 3GPP has delivered EDGE Evolution as part of Release 7, designed to complement High Speed Packet Access (HSPA), increasing throughput speeds to 1.3 Mbps in the downlink and 653 kbps in the uplink [5].

In 2000, the ITU initiative on IMT-2000 (International Mobile Telecommunications 2000), driven by the ambition for higher bandwidth, paved the way for evolution to Third Generation (3G). It were published a set of requirements such as a peak data rate of 2 Mb/s and support for vehicular mobility. Both the GSM and CDMA2000 camps formed their own separate 3G partnership projects (3GPP and 3GPP2, respectively) to develop IMT-2000 compliant standards based on the CDMA technology. The 3G standard in 3GPP is referred to as Wideband CDMA (W-CDMA) because it uses a larger 5 MHz bandwidth relative to 1.25 MHz bandwidth used in 3GPP2's cdma2000 system. The 3GPP2 also developed a 5 MHz version supporting three 1.25 MHz subcarriers referred to as cdma2000-3x. In order to differentiate from the 5 MHz system (entitled cdma2000-3x standard) the 1.25 MHz system is referred to as cdma2000-1x or simply 3G-1x.

You must be asking yourself why cdma2000-1×RTT belongs to the Second Generation. The first releases of the 3G standards did not fulfill its promise of high speed data transmissions because the data rates supported in practice were much lower than that claimed in the standards. This was the reason behind some of these technologies are considered Second Generation technologies. A serious effort was then made to enhance the 3G systems for efficient data support. The 3GPP2 first introduced the HRPD (High Rate Packet Data) [7] system that used various advanced techniques optimized for data traffic such as channel sensitive scheduling, fast link adaptation and hybrid ARQ, etc. The HRPD system required a separate 1.25 MHz carrier and supported no voice service. This was the reason that HRPD was initially referred to as cdma2000-1xEVDO (Evolution Data Optimized) system. The 3GPP followed a similar path and introduced HSPA (High Speed Packet Access) [8] enhancement to the W-CDMA system.

The HSPA standard reused many of the same data optimized techniques as the HRPD system. A difference relative to HRPD, however, is that both voice and data can be carried on the same 5 MHz carrier in HSPA. In parallel to HRPD, 3GPP2 also developed a joint voice data standard that was referred to as cdma2000-1xEVDV (Evolution Data Voice) [9]. Like HSPA, the cdma2000-1xEVDV system supported both voice and data on the same carrier but it was never commercialized. In the later release of HRPD, VoIP (Voice over Internet Protocol) capabilities were introduced to provide both voice and data service on the same carrier. The two 3G standards namely HSPA and HRPD were finally able to fulfill the 3G promise and have been widely deployed in major cellular markets to provide wireless data access.

While HSPA and HRPD systems were being developed and deployed, IEEE 802 LMSC (LAN/MAN Standard Committee) introduced the IEEE 802.16e standard [10] for mobile broadband wireless access. This standard was introduced as an enhancement to an earlier IEEE 802.16 standard for fixed broadband wireless access. The 802.16e standard employed a different access technology

named OFDM (Orthogonal Frequency Division Multiplexing) and claimed better data rates and spectral efficiency than that provided by HSPA and HRPD. Although the IEEE 802.16 family of standards is officially called WirelessMAN in IEEE, it has been dubbed WiMAX (Worldwide Interoperability for Microwave Access) by an industry group named the WiMAX Forum. The mission of the WiMAX Forum is to promote and certify the compatibility and interoperability of broadband wireless access products. The WiMAX system supporting mobility as in IEEE 802.16e standard is referred to as Mobile WiMAX. In addition to the radio technology advantage, Mobile WiMAX also employed a simpler network architecture based on IP protocols.

The introduction of Mobile WiMAX led both 3GPP and 3GPP2 to develop their own version of beyond 3G systems based on the OFDM technology and network architecture similar to that in Mobile WiMAX. The beyond 3G system in 3GPP is called Evolved Universal Terrestrial Radio Access (E-UTRA) [11] and is also widely referred to as LTE (Long-Term Evolution), while 3GPP2's version is called UMB (Ultra Mobile Broadband) [12].

2.2. Long-Term Evolution

As we known, HSPA and its evolution are strongly positioned to be the dominant mobile data technology for the next decade, however the GSM family of standards must evolve toward the future. Long Term Evolution (LTE) is part of the GSM evolutionary path beyond the 3G technology, following EDGE, UMTS, HSPA (HSDPA and HSUPA combined) and HSPA Evolution (HSPA+).

LTE's study phase began at 3GPP in late 2004. Two years later, the LTE of the 3rd generation radio access technology (E-UTRA) progressed from the feasibility study stage to the first issue of approved technical specifications. In December 2008, the specifications were sufficiently stable for commercial implementation and Release 8 was frozen [5].

LTE's project focused on enhancing the Universal Terrestrial Radio Access (UTRA) and optimizes 3GPP's radio access architecture to support packet-switched traffic. Within the formal 3GPP specifications, the LTE evolved radio access network is split into two parts: the Evolved UMTS Terrestrial Radio Access (E-UTRA) describing the radio evolution; and the Evolved UMTS Terrestrial Radio Access Network (E-UTRAN) for the core network evolution. For simplicity, this thesis refers to the new air interface by its project name, LTE. This name became common usage just as happened with another project name, UMTS, which has been synonymous with W-CDMA since 1999. The overall goal was to select technology that would keep 3GPP's Universal Mobile Telecommunications System (UMTS) at the forefront of mobile wireless well into the next decade.

The key project objectives were set in the following areas [5] [13] [14]:

- User demand for higher data rates (peak and average data throughput);

- Spectral efficiency;

- Minimal latency;

- Quality of service (QoS);

- Flexible channel bandwidths;

- Avoid unnecessary fragmentation of technologies for paired and unpaired band operation;

- Packet Switch optimized system;

- Seamless mobility;

- Low complexity;

- Continued demand for cost reduction (CAPEX and OPEX);

- Need to ensure the continuity of competitiveness of the 2G and 3G system for the future.

To fulfill all needs, the main decision was whether to pursue the objectives by continuing to evolve the existing W-CDMA air interface (which incorporates HSPA[3]) or adopt a new air interface based on OFDM. At the conclusion of the study phase, 3GPP decided that the project objectives could not be entirely met by evolving HSPA. As a result, the LTE evolved radio access network (E-RAN) is based on a completely new OFDM air interface. OFDM is an attractive choice to meet requirements for high data rates, with correspondingly large transmission bandwidths and flexible spectrum allocation. OFDM also allows for a smooth migration from earlier radio access technologies and is known for high performance in frequency selective channels. It further enables frequency domain adaptation, provides benefits in broadcast scenarios, and is well suited for Multiple Input Multiple Output (MIMO) processing. MIMO technology to beyond to provide even higher peak data rates, also support 10 times the users per cell as 3GPP's original W-CDMA radio access technology [5].

---

[3] HSPA (high-speed packet access) refers collectively to high-speed downlink packet access (HSDPA) and high-speed uplink packet access (HSUPA), the latter being formally known as the Enhanced Dedicated Channel (E-DCH).

Nevertheless, LTE uses others technologies derived from OFDM, Orthogonal Frequency Division Multiple Access (OFDMA) was selected for the Downlink, and Single Carrier-Frequency Division Multiple Access (SC-FDMA) for the Uplink. OFDMA is well suited to achieve high peak data rates in high spectrum bandwidth, however, a pure OFDMA approach results in high peak-to-average power ratio (PAPR) of the signal, which compromises power efficiency and, ultimately, battery life. Hence, on the uplink, LTE uses an approach for the uplink called SC-FDMA, which is somewhat similar to OFDMA, but has a 2 to 6 dB PAPR advantage over the OFDMA method [16]. This is an advantage when compared with other technologies, such as WiMAX IEEE 802.16e, that use OFDM in both stream directions.

The standard supports a number of digital modulation schemes for the transmission of data. The four main modulations supported by LTE are BPSK, QPSK, 16QAM and 64QAM. The downlink supports data modulation schemes QPSK, 16QAM, and 64QAM and the Uplink BPSK, QPSK and 16QAM [5]. Each modulation is capable of an increasingly higher bit rate at the expense of being less robust and more susceptible to signal errors and path loss. Figure 2 illustrates the modulations selected by LTE depending on the signal-to-noise ratio (SNR) (it is assumed, for the sake of simplicity, that a greater distance results in a lower SNR).
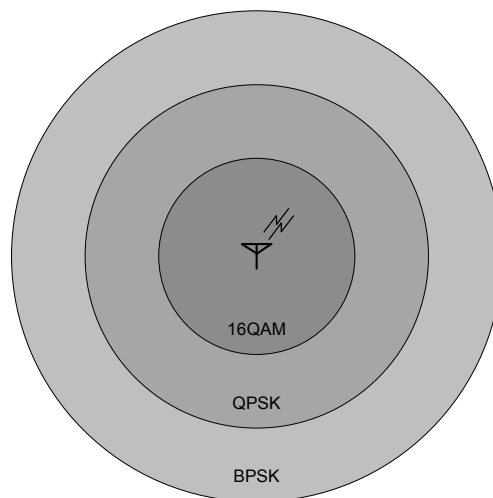
Figure 2 - Diagram of LTE UL selection of schemes modulation

The possibility to operate in vastly different spectrum allocations is essential. LTE E-UTRA is also highly flexible in channelization, so a scalable number of defined channel bandwidths are used. Spectrum allocations supported are ranging from 1.25 to 20 MHz (1.4, 3, 5, 10, 15 and 20 MHz), contrasted with UTRA's fixed 5 MHz channels. Different bandwidths are realized by varying the number of subcarriers used for transmission, while the subcarrier spacing remains unchanged.

LTE also boosts spectral efficiency, increased up to four-fold compared with UTRA. Due to the fine frequency granularity offered by OFDM (only 15 kHz of subcarrier spacing), a smooth migration of 2G/3G spectrum is possible using only a fraction of the available OFDM subcarriers. In others words, LTE can co-exist with earlier 3GPP radio technologies, even in adjacent channels, and calls can be handed over to and from all 3GPP's previous radio access technologies. Frequency-division duplex (FDD), time-division duplex (TDD), and combined FDD/TDD [17], to separate DL and UL traffic, allow the operation in paired as well as unpaired spectrum, as illustrated in Figure 3.
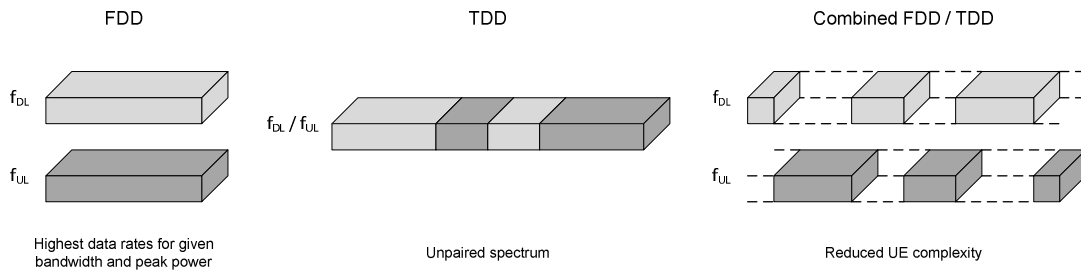
Figure 3 - Duplex schemes [17]

The targets were to have average user throughput of three to four times the Release 6 HSDPA levels in the Downlink (100 Mbps), and two to three times the HSUPA levels in the Uplink (50 Mbps), allowing to bring many technical benefits to cellular networks [5]. W-CDMA radio technology is, essentially, as efficient as OFDM for delivering peak data rates of about 10 Mbps in 5 MHz of bandwidth. Achieving peak rates in the 100 Mbps range with wider radio channels, although it would result in highly complex terminals and is not practical with current technology. This is where OFDM provides a practical implementation advantage, and by using OFDM, LTE is aligning with similar decisions made by 3GPP2 for Ultra Mobile Broadband (UMB) and by IEEE 802.16 for WiMAX.

LTE is, undoubtedly, the future technology for cellular networks. However, this does not mean the end of 3GPP's interest in GSM and W-CDMA. Rather, the investment in these technologies and their remaining potential untapped mean that LTE is not the only format being developed in 3GPP Release 8. For example, the EDGE Evolution project will be pushing GSM to newer levels and the HSPA+ project will continue to evolve the underlying W-CDMA, HSDPA and HSUPA technologies. These features will suit the needs of different network operators that have different bandwidth allocations, and also allow operators to provide different services based on spectrum [2].

In addition to developing LTE, 3GPP also worked on a complementary project known as System Architecture Evolution (SAE), which defines the split between LTE and a new Evolved Packet Core (EPC), optimizing architecture and signalling for packet mode and in particular for the IP-

Multimedia Subsystem (IMS), which supports all access technologies. This is a flatter packet-only core network that aims to deliver higher throughput, lower cost and reduce round-trip latency, providing capabilities for less than 10 ms latency for the transmission of a packet from the network to the user equipment. The EPC is also designed to provide seamless interworking with existing 3GPP and non-3GPP access technologies. This topic will be completed in next section. Table 1 shows the main features of LTE. Some of the issues covered here will be studied in detail in the following chapters.

Table 1 - LTE system attributes [1]

	Downlink	Uplink
Bandwidth	1.25 – 20 MHz	
Duplexing	FDD, TDD, half-duplex FDD	
Mobility	Optimized mode	0 - 15 km/h
	High performance mode	15 - 120 km/h
	Functional mode	120 - 350 km/h
Multiple access	OFDMA	SC-FDMA
Peak rate in 20 MHz (theoretical values)	100 Mbps (1×1 / 64QAM)	50 Mbps (1×1 / QPSK)
	172.8 Mbps (2×2 / 64QAM)	57.6 Mbps (1×1 / 16QAM)
	326 Mbps (4×4 / 64QAM)	86.4 Mbps (1×1 / 64QAM)
Specified Modulation	QPSK, 16QAM and 64QAM	BPSK, QPSK and 16-QAM
Channel coding	Turbo code	
Latency	< 10 ms	
Other techniques	Channel sensitive scheduling	
	Link adaptation	
	Power control	
	ICIC	
	Hybrid ARQ	

Standards development for LTE continued with 3GPP Release 9 (finished in December 2009). 3GPP recognized the need to develop a solution and specification to be submitted to the International Telecommunication Union (ITU) for meeting the IMT-Advanced requirements (4G). Therefore, in parallel with Release 9 work, 3GPP worked on a study item called LTE-Advanced [15], which defines the bulk of the content for Release 10 (finished in March 2011), and include significant new technology enhancements to LTE/EPC [5]. Actually, 3GPP continues to study further advancements for the E-UTRAN with work already in progress at 3GPP in Release 11.

2.3. Network architecture

System Architecture Evolution (SAE) is the network architecture of 3GPP's LTE. The main component of the SAE architecture is the Evolved Packet Core (EPC). SAE/EPC is defined by 3GPP in Release 8 as an entirely new core network with the goal of supporting flatter all-IP architecture, enabling higher data rate, seamless mobility, quality of service (QoS) and lower latency. 3GPP has targeted user-plane latency at 10 ms. It also supports multiple heterogeneous access networks, including E-UTRA (LTE and LTE-Advanced air interface), 3GPP legacy systems (GERAN and/or UTRAN networks connected via SGSN) and non-3GPP systems focusing on the packet-switched domain (e.g. WiMAX or cdma2000). Further, the packet-switched approach allows supporting all services via IP including voice through packet connections [16].

Through the SAE work item, 3GPP has made a significant progress in Release 8 towards the standards development and definition of a new flatter-IP core network to support the Evolved UMTS Terrestrial Radio Access Network (E-UTRAN), which has recently been renamed the Evolved Packet Core (EPC) Architecture [19]. The result is a simplified architecture with only two network elements, called evolved NodeB (eNodeB) and Access Gateway (AGW), see Figure 4. One major change is that the radio network controller (RNC) is eliminated from the data path, so eNodeB integrates the functions traditionally performed by the radio network controller (RNC). This is in contrast to many more network nodes in the current hierarchical network architecture of the 3G system, where a separate node controlled multiple NodeB. Some of the benefits of a single node in the access network are reduced latency and the distribution of the RNC processing load into multiple eNodeB. The elimination of the RNC in the access network was possible partly because the LTE system does not support macro-diversity or soft-handoff. Meanwhile, the AGW integrates the functions traditionally performed in UTRAN by the SGSN and GGSN. The AGW has both control functions, handled through the Mobile Management Entity (MME), and user plane (data communications) functions. The MME supports user equipment context and identity, as well as authenticating and authorizing users. The user plane functions consist of two elements, a Serving Gateway (S-GW) that addresses 3GPP mobility and terminates eNodeB connections, and a Packet Data Network Gateway (PDN-GW) that addresses service requirements (controls IP data services, does routing, allocates IP addresses and enforces policy) and provides access for non-3GPP access networks. The MME serving gateway and PDN gateways can be collocated in the same physical node or distributed. EPC architecture also supports Policy Control and Charging Rules Function (PCRF) that manages QoS aspects. Note that the complete packet system consisting of the E-UTRAN/LTE and the SAE/EPC is called the Evolved Packet System (EPS) [18].
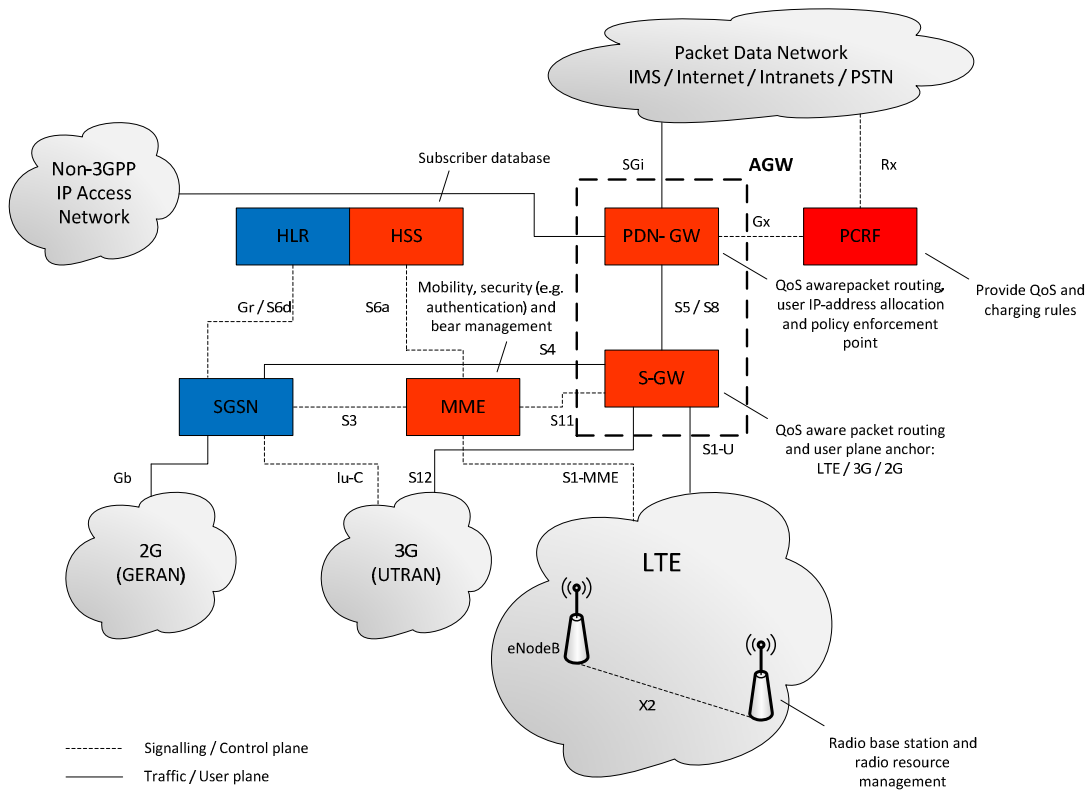
Figure 4 - Evolved Packet System

The combination of LTE and SAE/EPC provides the long term vision for 3GPP, OFDM radio system and packet switching optimization performed improve the performance, providing higher data rates and reduced latency. This is particularly important today when all application services require greater bandwidth with low delay times. It's a matter of time until mobile operators to add the HSPA + and LTE to their radio access networks, simultaneously, they will evolve the rest of their networks and subscriber devices and they will beef up their core and backhaul networks to handle the exponential increases in IP traffic enabled by HSPA+ and LTE. To keep their networks performing optimally, mobile operators will flatten their core network architectures considerably by using EPC technology. So, as we saw earlier, EPC reduces the number of nodes in the core, which reduces latency even as the amount of data traffic increases. It simplifies deployment of IP-based networks and reduces the cost of their deployments [16].

EPC will use IP Multimedia Subsystem (IMS) as a component. It will also manage Quality of Service (QoS) across the whole system, which will be essential for enabling a rich set of multimedia-based services. The EPS will be optimized for all services to be delivered via IP in a manner that is as efficient as possible, through minimization of latency within the system, for instance. The QoS architecture in EPC enables a number of important capabilities for both operators and users:

- VoIP support with IMS. QoS is a crucial element for providing LTE/IMS voice service;

- Enhanced application performance. Applications such as gaming or video can operate more reliably;

- More flexible business models. With flexible, policy-based charging control, operators and third-parties will be able to offer content in creative new ways. For example, an enhanced video stream to a user could be paid for by an advertiser;

- Congestion control. In congestion situations, certain traffic flows (e.g. bulk transfers, abusive users) can be throttled down to provide a better user experience for others.

Although it will most likely be deployed in conjunction with LTE, EPC may also be deployed for use with HSPA+, where it would provide a stepping-stone to LTE. It will support service continuity across heterogeneous networks, important for LTE operators that must simultaneously support GSM/GPRS/EDGE/UMTS/HSPA customers [18].

2.4. Summary

For many years now, a true world cellular standard has been one of the industry's goals. GSM dominated second generation (2G) technologies but there was still fragmentation with CDMA and TDMA. With the move to third generation (3G), the historical divide remained between GSM and CDMA. The opportunity has arisen for a global standard technology with the next step of technology evolution. Now, many operators have converged on the technology they believe will offer them and their customers the most benefits. That technology is Long Term Evolution. For the first time, all GSM and CDMA operators are walking towards global consensus.

LTE assumes a full Internet Protocol (IP) network architecture and is designed to support voice in the packet domain. It also incorporates new radio access techniques, such as OFDM, SC-FDMA, MIMO, etc., to achieve an extremely high performance levels beyond what will be practical with CDMA approaches, particularly in larger channel bandwidths, offering full vehicular speed mobility. However, in the same way that 3G coexists with second generation (2G) systems in integrated networks, LTE systems will coexist with 3G and 2G systems. Multimode devices can function across LTE/3G or even LTE/3G/2G.

Then, we summarize the technical reports [5], [15] and [20] that contains detailed requirements and specifications for the following criteria:

Table 2 - Key features of LTE Release 8

User throughput	OFDM technology in Downlink	Robust against multipath interference.
		High affinity to advanced techniques, such as frequency domain channel-dependent scheduling.
		Multi-antenna schemes (1x1, 2x1, 2x2, 4x2, 4x4).
		Peak data rates 3 to 4 times Release 6 HSDPA (up to 100 Mbps within 20 MHz downlink spectrum allocation for SISO systems 64QAM modulation).
	SC-FDMA technology in Uplink	Low PAPR.
		User orthogonality in frequency domain.
		Multi-antenna schemes (1x1, 1x2).
		Peak data rates 2 to 3 times Release 6 HSUPA (up to 50 Mbps within 20 MHz uplink spectrum allocation for SISO systems and QPSK modulation).
Spectrum flexibility	E-UTRA shall operate in spectrum allocations of different sizes, including support to scalable bandwidths of 1.4, 3, 5, 10, 15 and 20 MHz in both the uplink and downlink.	
	The system shall be able to support content delivery over an aggregation of resources including Radio Band Resources (as well as power, adaptive scheduling, etc.) in the same and different bands, in both uplink and downlink, and in both adjacent and non-adjacent channel arrangements. A "Radio Band Resource" is defined as all spectrum available to an operator.	
Spectrum efficiency	Downlink	In a loaded network, spectrum efficiency (bits/sec/Hz/site) is 3 to 4 times Release 6 HSDPA (5 bps/Hz).
	Uplink	In a loaded network, spectrum efficiency (bits/sec/Hz/site) is 2 to 3 times Release 6 HSUPA (2.5 bps/Hz).
User and Control plane latency	Short transfer delay, up to 10 ms round-trip times between user equipment and the base station, and less than 5 ms in unload condition (i.e. single user with single data stream) for small IP packet.	
	Short setup time, less than 100 ms transition times from inactive to active.	
	Short handover latency and interruption time and short TTI.	

Spectrum arrangement	FDD and TDD within a single radio access technology (operation in paired and unpaired spectrum).		
Further enhanced Multimedia Broadcast Multicast Service (MBMS)	Support for MBSFN (Multicast Broadcast Single Frequency Network) for efficient Multicast/Broadcasting using single frequency network by OFDM.		
Architecture	Single E-UTRAN architecture	eNodeB as the only E-UTRAN node.	
		Smaller number of RAN interfaces: eNodeB » MME/SAE-Gateway (interface: S1) eNodeB » eNodeB (interface: X2)	
	Simple protocol architecture	Shared channel based.	
		Packet switch mode only with VoIP capability.	
	The E-UTRAN architecture shall be packet based, although provision should be made to support systems supporting real-time and conversational class traffic.		
	E-UTRAN architecture shall minimize the presence of "single points of failure".		
	E-UTRAN architecture shall support an end-to-end QoS.		
	Support of load sharing and policy management across different radio access technologies.		
	Support of Self-Organising Network (SON) operation.		
Co-existence and Inter-working with other technologies	Co-existence in the same geographical area with legacy standards and co-location with GERAN/UTRAN on adjacent channels.		
	E-UTRAN terminals supporting also UTRAN and/or GERAN operation should be able to support measurement of, and handover from and to, both 3GPP UTRAN and 3GPP GERAN.		
	The interruption time during a handover of real-time services between E-UTRAN and UTRAN (or GERAN) should be less than 300 ms.		
	Compatibility and inter-working with earlier 3GPP radio access technologies (e.g. GSM and HSPA).		
	Inter-working with others radio access technologies (e.g. cdma2000).		
eNodeB capacity	At least 200 users per cell should be supported in the active state for spectrum allocations up to 5 MHz.		
eNodeB Coverage	Throughput, spectrum efficiency and mobility targets can be met for 5 km cells, and with slight degradation for 30 km cells. Cells with a range up to 100 km are also supported with acceptable performance.		

Mobility	E-UTRAN is optimized with full performance for low mobile speed up to 15 km/h.
	Higher mobile speed between 15 and 120 km/h support high performance with slight degradation.
	Mobility across the cellular network shall be maintained at speeds from 120 km/h to 350 km/h (or even up to 500 km/h depending on the frequency band used).
Complexity	Minimize the number of options.
	No redundant mandatory features.

Chapter 3

3. Multicarrier Systems

Orthogonal Frequency Division Multiplexing (OFDM) is the multicarrier system used in LTE technology, which it aims achieve frequency diversity through the use of multicarrier modulation. OFDM systems transmit information data in many subcarriers, where subcarriers are orthogonal to each other, so that the spectrum efficiency may be enhanced. OFDM can be easily implemented by the IFFT (inverse fast Fourier transform) and FFT (fast Fourier Transform) process in digital domain, and has properties such as high-speed broadband transmission, robustness to multipath interference, frequency selective fading and high spectral efficiency. It is also worth mentioning that the OFDM modulation scheme can be used to make a multiple access techniques, resulting in Orthogonal Frequency Division Multiple Access (OFDMA) and Single-Carrier Frequency Division Multiple Access (SC-FDMA). Figure 5 shows how a series symbols are mapped into time and frequency by the two different modulation schemes.
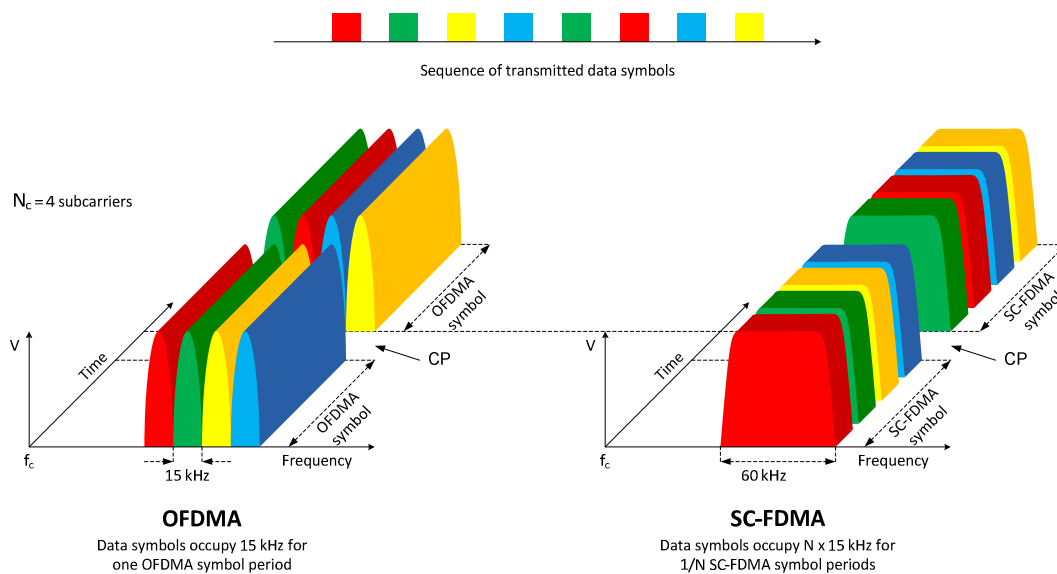

Figure 5 - Comparation of how OFDMA and SC-FDMA transmit a sequence of data symbols [2]

In this chapter, we will look into a novel commercial modulation system used in LTE, which aims transmit information data in many subcarriers. We begin with a thorough description over the OFDM modulation principles, in Section 3.1. Then, we continue with its adaptation to a multiple

access techniques, OFDMA and SC-FDMA, in Section 3.2 and 3.3, respectively. The reader that wants to broaden its knowledge with respect to these topics is referred to [1] and [21].

3.1. Orthogonal Frequency Division Multiplexing

OFDM can be viewed as a form of Frequency Division Multiplexing (FDM) with the special property that each carrier is orthogonal with every other carrier, but it is different from FDM in several ways. First, FDM requires, typically, the existence of frequency guard bands between the frequencies, so that they do not interfere with each other. Unlike, OFDM allows the spectrum of each carrier is overlapped because as they are orthogonal and they not interfere with each other. Furthermore, the overall amount of required spectrum is reduced due to the overlapping of the carriers.

In OFDM, a subcarrier spacing of 15 kHz is adopted, allowing be compatible with other radio access technologies and coverage larger areas of network with a single antenna. To minimize delays, the subframe duration is selected as short as 0.5 ms, corresponding to two slots of seven OFDM symbols. The cyclic prefix length of 4.67 µs is sufficient for handling the delay spread for most unicast scenarios, while only adding modest overhead. Very large cells with large amounts of time dispersion are handled by reducing the number of OFDM symbols in each slot by one in order to extend the cyclic prefix to 16.67 µs. Broadcast services are supported by transmitting the same information from multiple (synchronized) base stations. For the mobile terminal, the received signal from all base stations will appear as multipath propagation and thus implicitly be exploited by the OFDM receiver [17].

OFDM provide a substantial increase in spectral efficiency by exploiting channel variations in the time domain through link adaptation and channel dependent scheduling, as is done in current 3G's systems, such as W-CDMA and HSPA. With the evolved radio access, this is taken one step further by adapting the transmission parameters not only in the time domain, but also in the frequency domain. Frequency domain adaptation is made possible through the use of OFDM and can achieve large performance gains in cases where the channel varies significantly over the system bandwidth. Thus, frequency domain adaptation becomes increasingly important with an increasing system bandwidth. Information about the channel quality, obtained through feedback from the terminals, is provided to the scheduler allocate to which user and dynamically selects an appropriate data rate for each chunk by varying the output power level, the channel coding rate, and/or the modulation scheme (BPSK, QPSK, 16-QAM and 64-QAM) [21].

Then, let's peel some aspects that we consider most important in OFDM.

3.1.1. Multicarrier Modulation

In a single carrier modulation system, the data is sent serially over the channel by modulating one single carrier at a baud rate of R symbols per second. The data symbol period is $T_{symbol} = 1/R$.

The basic idea of the multicarrier modulation is, nevertheless, that the available bandwidth, W, is divided into a number N_c of sub-bands, commonly called subcarriers. As shown in Figure 6, each one of these subcarriers has a width of $\Delta f = W/N_c$. Instead of transmitting the data symbols in a serial way at a baud rate R, a multicarrier transmitter partitions the data stream into blocks of N_c data symbols and those are transmitted in parallel by modulating the N_c subcarriers. The symbol duration for a multicarrier scheme is then $T_{symbol} = N_c/R$.
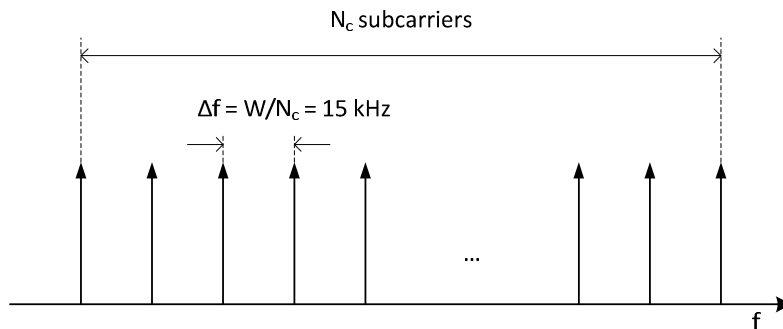
Figure 6 - Subdivision of the bandwidth into Nc sub-bands (multicarrier transmission)

One of the main advantages of using a multicarrier modulation is that inter-symbol interference (ISI) can be reduced when the number of subcarriers, N_c, increases. In a multipath fading channel, ISI can appear due to the fact that the time dispersion is significant when compared with the symbol period. If a single carrier modulation is used, a complex equalizer for compensating the channel distortion is needed. However, the multicarrier modulation simplifies the equalization into single multiplications in the frequency domain [21]. This issue will be discussed in more detail in Chapter 5.

3.1.2. Orthogonality

In order to assure a high spectral efficiency, the carrier waveform must be composed by overlap of several transmit spectra. Nevertheless, to enable a simple separation of these overlapping subcarriers at the receiver they need to be orthogonal.

Orthogonality is a property that allows the signals to be perfectly transmitted over a common channel and detected without interference. However, loss of orthogonality results in blurring between these information signals and degradation in communication.

Set of functions are orthogonal to each other if they match the conditions in Equation 3.1. It means that if any two different functions within a set are multiplied and integrated over a symbol period, the result is zero for orthogonal functions.

$$\int_0^T S_i(t).S_j(t)dt = \begin{cases} C & i = j \\ 0 & i \neq j \end{cases} \tag{3.1}$$

Each OFDM subcarrier has a sinc(x)[4] frequency response. This is the result of the symbol time corresponding to the inverse of the carrier spacing. The sinc(x) shape has a narrow main lobe with many side lobes that decay slowly with the magnitude of the frequency difference away from the centre. Each carrier has a peak at its centre frequency and nulls evenly spaced with a frequency gap equal to the carrier spacing [21].

The orthogonal nature of the transmission is a result of the peak of each subcarrier corresponding to the nulls of all other subcarriers, as shown in Figure 7.
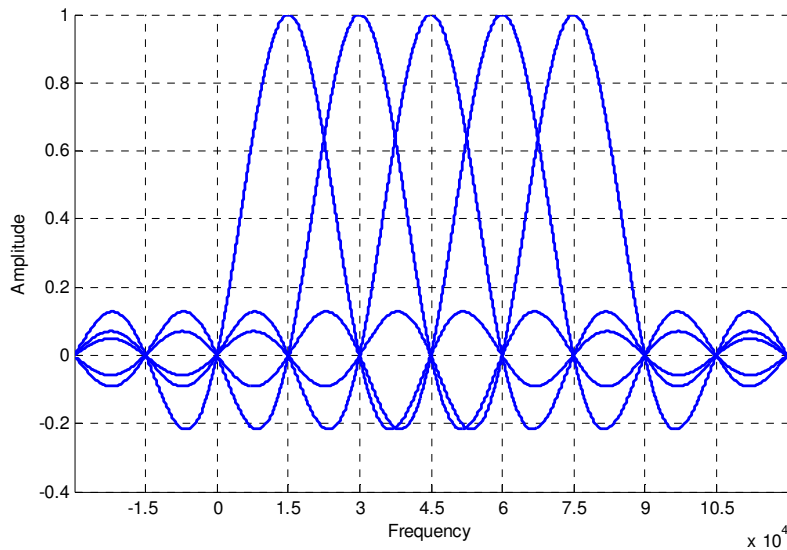

Figure 7 - Spectrum of an OFDM signal

---

[4] sinc(x) = sin(x)/x

3.1.3. Cyclic Prefix

Passing the signal through a time-dispersive channel causes ISI. In an OFDM system, a loss of the orthogonality appears due to ISI, resulting in inter-carrier interference (ICI). For a given system bandwidth the symbol rate for an OFDM signal is much lower than a single carrier transmission scheme. It is because the OFDM system bandwidth is broken up into N_c subcarriers resulting in a symbol rate that is N_c times lower. This low symbol rate makes OFDM naturally resistant to effects of ISI caused by multipath propagation.

The multiple signals that appear due to the multipath propagation arrive at the receiver at different times, spreading the symbol boundaries and causing energy leakage between the OFDM symbols. Furthermore, in an OFDM signal the amplitude and phase of the subcarrier must remain constant over a period of the symbol in order to maintain the orthogonality of the subcarriers. If they are no constant, the spectral shape will not have nulls at the correct frequencies, resulting in ICI.

In order to combat the effects of ISI on an OFDM signal, a guard period to the start of each symbol is added. This guard period, which is called the cyclic prefix (CP), is a copy of the last part of the OFDM symbol, thus extending the length of the symbol waveform [21]. Figure 8 shows the structure of an OFDM symbol.
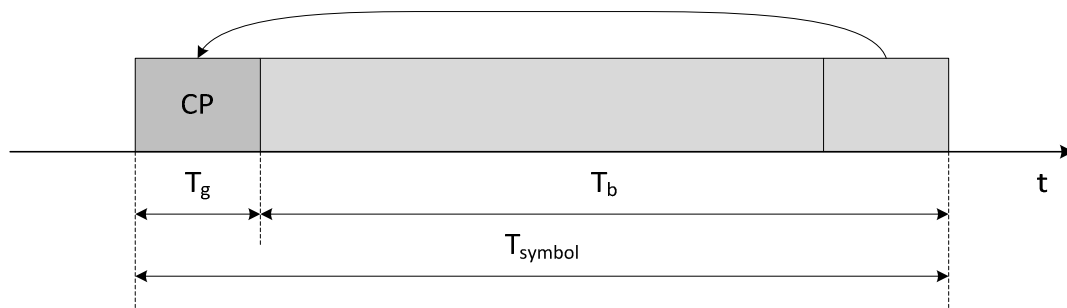
Figure 8 - Addition of the cyclic prefix to an OFDM signal

The CP is prepended to the transmitted symbol and removed at the receiver before the demodulation. Then, the total length of the symbol can be written as

$$T_{symbol} = T_g + T_b \tag{3.2}$$

where T_{symbol} is the total length of the symbol in samples, T_g is the length of the guard period in samples, and T_b is the size of the IFFT used to generate the OFDM signal, representing the useful symbol time. Note that, the CP duration is described in absolute terms (e.g. 16.67 μs for long CP)

and in terms of standard time units, T_s, that is used throughout the LTE specification documents. For instance, it is defined as $T_s = 1/(1500 \times 2048) = 32.55\,\mu s$, which corresponds to the 30.72 MHz sample clock for the 2048 point FFT used with the 20 MHz system bandwidth.

Consequently, the benefit obtained for the addition of a cyclic prefix is twofold. First, it avoids ISI acting as a guard band between two successive symbols. Seconds, it converts the linear convolution with the channel impulse response into a cyclic convolution. However, the length of the cyclic prefix has to be chosen carefully. It should be, at least, as long as the significant part of the impulse response experienced by the transmitted signal, allowing some time for the transient signal to decay, and thus, avoiding ISI and ICI, and it should be as small as possible because the transmitted energy increases with its length, causing a loss in the SNR. Equation 3.3 gives the SNR loss due to the insertion of the CP. Moreover, the number of symbols per second that are transmitted per Hertz of bandwidth also decreases with the CP. The decreasing coefficient is expressed by $\left(1 - T_g/T_{sysmbol}\right)$.

$$
\begin{cases}
SNR_{loss} = \dfrac{P_{signal}}{P_{noise}} = \dfrac{P_{signal}}{P_{signal}\left(1 - \frac{T_g}{T_{symbol}}\right)} = \dfrac{T_{symbol}}{T_{symbol} - T_g} \\
\qquad\qquad or \\
SNR_{loss} = -10log_{10}\left(1 - \dfrac{T_g}{T_{symbol}}\right)\,[db]
\end{cases}
\tag{3.3}
$$

In other words, the system performance is 93.4% or 80% when it used short CP and long CP, respectively.

$$
Short\ CP\ \rightarrow
\begin{cases}
SNR_{loss} = \dfrac{4.69 + 66.67}{4.69 + 66.67 - 4.69} = 1.0708 \\
\eta = SNR_{loss}^{-1} = \dfrac{1}{1.0708} = 0.934\ (93.4\%)
\end{cases}
$$

$$
Long\ CP\ \rightarrow
\begin{cases}
SNR_{loss} = \dfrac{16.67 + 66.67}{16.67 + 66.67 - 16.67} = 1.25 \\
\eta = SNR_{loss}^{-1} = \dfrac{1}{1.25} = 0.8\ (80\%)
\end{cases}
$$

3.1.4. Generic Frame Structure

One element shared by the LTE DL and UL is the generic frame structure. In OFDM, users are allocated in a specific number of subcarriers for a predetermined amount of time. These are referred to as physical resource blocks (PRBs) in the LTE specifications. PRBs thus have both a time and frequency dimension. Allocation of PRBs is handled by a scheduling function at the 3GPP base station (eNodeB) and is the smallest element of resource allocation assigned by the base station

scheduler. Although it involves added complexity in terms of resource scheduling, it is vastly superior to packet-oriented approaches in terms of efficiency and latency [21].

In order to adequately explain OFDM within the context of the LTE, the generic frame structure is used with FDD. Alternative frame structures are defined for use with TDD, however, this alternative frame structures is not considered in this work.

As shown in Figure 9, LTE frames have duration of 10 ms and they are divided into 10 subframes of 1 ms in duration. Each subframe is further divided into two slots, each of 0.5 ms duration. As mentioned above section, slots consist of either 6 or 7 ODFM symbols, depending on whether long or short cyclic prefix is employed, respectively [24].
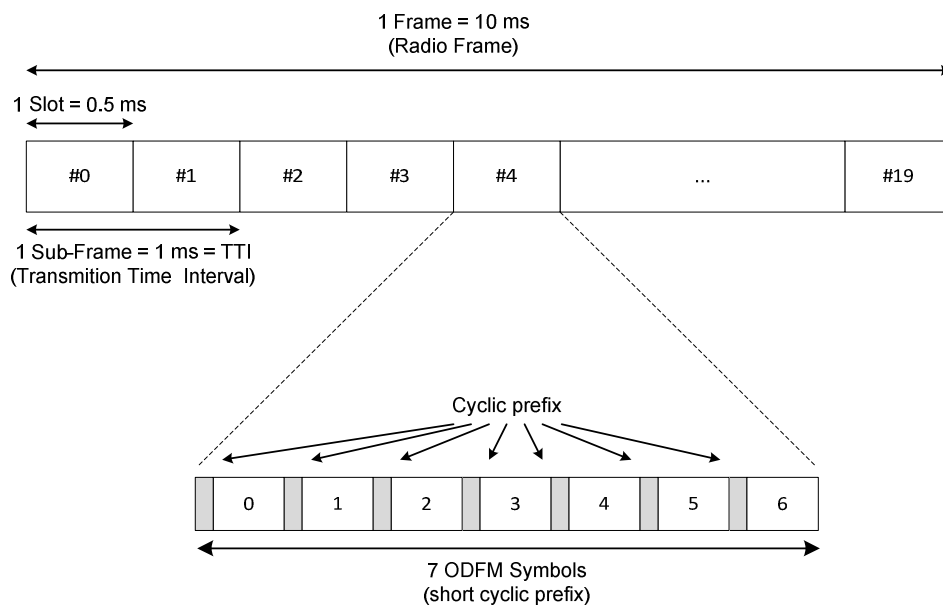
Figure 9 - LTE Generic Frame Structure (FDD frame structure)

Let's consider a specific LTE example. In the case of 1.25 MHz transmission bandwidth, the FFT size is 128. In other words, 128 samples are taken within the FFT period of 66.67 μs. Depending on the channel delay spread, either short or long CP is used. When short CP is used, a slot has seven consecutive OFDM symbols with CP duration of 4.67 μs ($7 \times 66.67 + 7 \times 4.69 \approx 500 \, \mu s$). On the other hand, when long CP is used, a slot has six consecutive OFDM symbols with CP duration of 16.7 μs ($6 \times 66.67 + 6 \times 16.67 \approx 500 \, \mu s$), as shown in Table 3. This is done to preserve slot timing of 0.5 ms.

Table 3 - OFDM Modulation Parameters of LTE Release 8

Access Scheme	Downlink	OFDMA					
	Uplink	SC-FDMA					
Bandwidth [MHz]		1.4	3	5	10	15	20
Number of available physical resource blocks (N_{RB})		6	12	25	50	75	100
Number of occupied subcarriers		72	180	300	600	900	1200
IDFT(TX)/DFT(RX) size		128	256	512	1024	1536	2048
Sampling frequency [MHz]		1.92	3.84	7.68	15.36	23.04	30.72
Samples per slot		960	1920	3840	7680	11520	15360
Minimum TTI		1 ms					
Subcarrier spacing		15 kHz					
Physical resource block bandwidth		180 kHz					
Subcarrier period		66.67 µs					
Slot duration		0.5 ms					
OFDM symbols per slot ($N_{Symbols}$)	Short CP	7 symbols					
	Long CP	6 symbols					
		3 symbols[5]					
Cyclic prefix length ($N_{CP,l}$) [samples]	Short CP	160 (≈5.21 µs) for l = 0					
		144 (≈4.69 µs) for l = 1, 2, …, 6					
	Long CP	512 (≈16.69 µs) for l = 0, 1, …, 5					
		1024 (≈33.33 µs)[5] for l =0, 1, 2					
Modulation		BPSK, QPSK, 16QAM, 64QAM					
Spatial multiplexing		Up to 4 layers for DL per UE					
		Single layer for UL per UE					
		MU-MIMO supported for DL and UL					

The total number of available subcarriers depends on the overall transmission bandwidth of the system. The LTE specifications define parameters for system bandwidths from 1.25 MHz to 20 MHz. A PRB is defined as consisting of 12 consecutive subcarriers (180 kHz) for one slot (0.5 ms) in duration. The transmitted signal consists of N_{BW} subcarriers with duration of $N_{\text{OFDM symbols}}$. It can be represented by a resource grid as depicted in Figure 10. Each box within the grid represents a single subcarrier for one symbol period and is referred to as a resource element.

---

[5] Δf = 7.5 kHz (only in downlink)
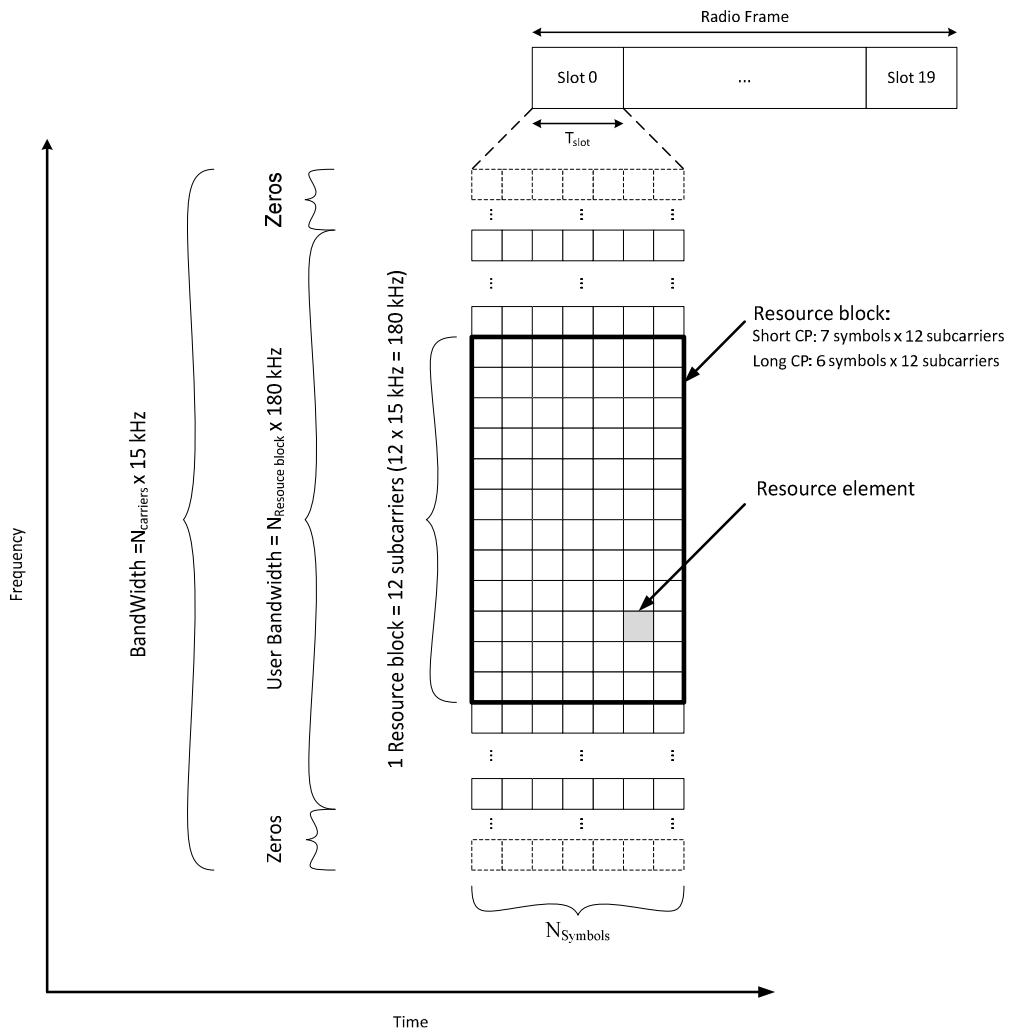
Figure 10 - LTE Resource Grid

In contrast to packet-oriented networks, LTE does not employ a PHY preamble to facilitate carrier offset estimate, channel estimation, timing synchronization etc. Instead, special reference signals are embedded in the PRBs, as shown in Figure 11.
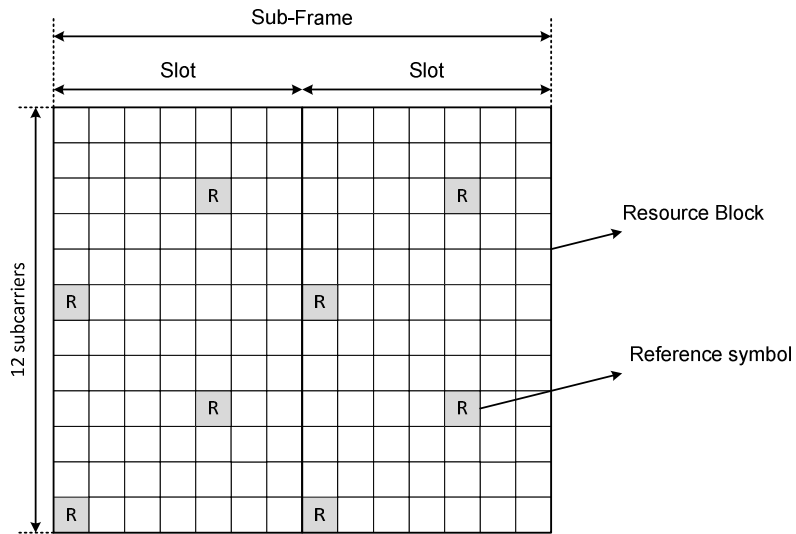
Figure 11 - LTE reference symbols

Reference signals are transmitted during the first and fifth OFDM symbols of each slot when the short CP is used and during the first and fourth OFDM symbols when the long CP is used [25]. In MIMO applications, there is a resource grid for each transmitting antenna, see Figure 12.
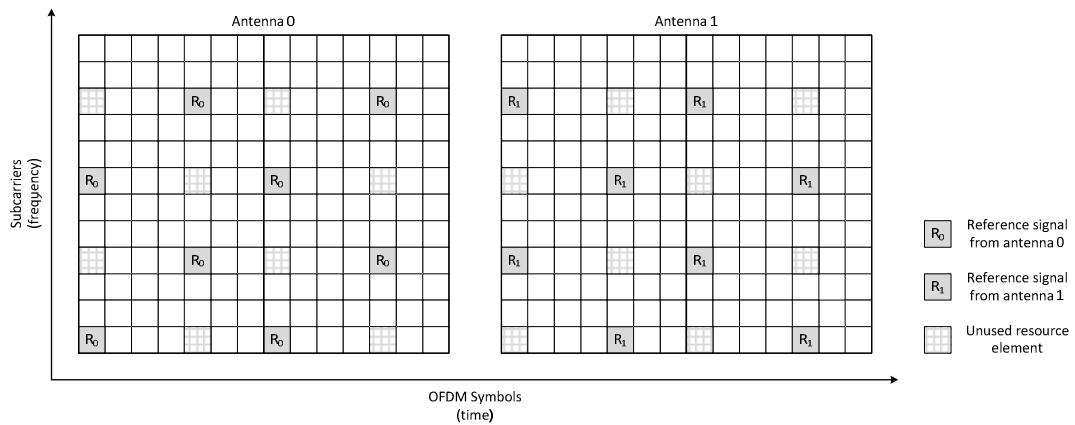
Figure 12 - Reference symbols for dual antenna

3.1.5. The OFDM system model

OFDM signals are typically generated digitally due to the difficulty in creating large banks of phase lock oscillators and receivers in the analog domain. Figure 13 shows the block diagram of an OFDM system. In the transmitter, the incoming data stream is grouped in blocks of N_c data symbols, which are the OFDM symbols, and can be represented by a vector x_m. Next, an IFFT is performed on each data symbol block and a cyclic prefix of length N_g is added.
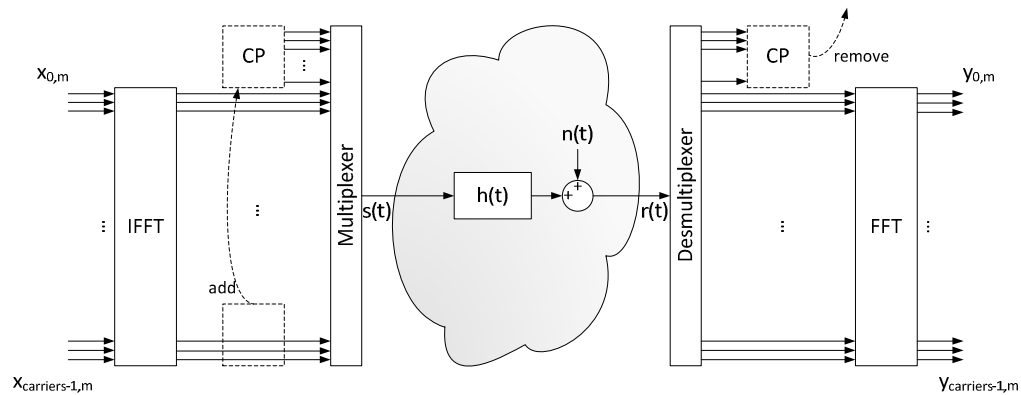
Figure 13 - Model of an OFDM system

The received signal is, generally, the sum of a linear convolution with the discrete channel impulse response, $h(n)$, and an additive white Gaussian noise, n(n). It has to be said that it is implicitly assumed that the channel fading is slow enough to consider it constant during one symbol, and both, transmitter and receiver, are perfectly synchronized. At the receiver, the cyclic prefix is removed, and then, the data symbol $y_{k,m}$ (frequency index k, OFDM symbol m) is obtained by performing the FFT operation.

Moreover, the transmitted data symbols, $x_{k,m}$, can be estimated from the received data symbols, $y_{k,m}$, using a single tap equalizer. This estimated symbol can be obtained easily by dividing each received data symbol by its corresponding channel coefficient. In Chapter 5 we will examine four different equalizers with different performances in terms of bit error rate (BER).

3.2. Orthogonal Frequency Division Multiple Access

OFDMA is the basic multiplexing scheme employed in the LTE downlink. Rather than using OFDM, we will now shift to the term OFDMA, which stands for Orthogonal Frequency Division Multiple Access. OFDMA is simply an elaboration of OFDM used by LTE and other systems that increases system flexibility by multiplexing multiple users onto the same subcarriers. This can benefit the efficient trunking of many low-rate users onto a shared channel as well as enable per-user frequency hopping to mitigate the effects of narrowband fading. OFDMA only differs from other systems such as UMB and WiMAX in details of the OFDM numerology (that is subcarrier spacing, symbol length, bandwidth, etc.). The basic time-frequency structure of the multiple access techniques of LTE are illustrated in Figure 14.
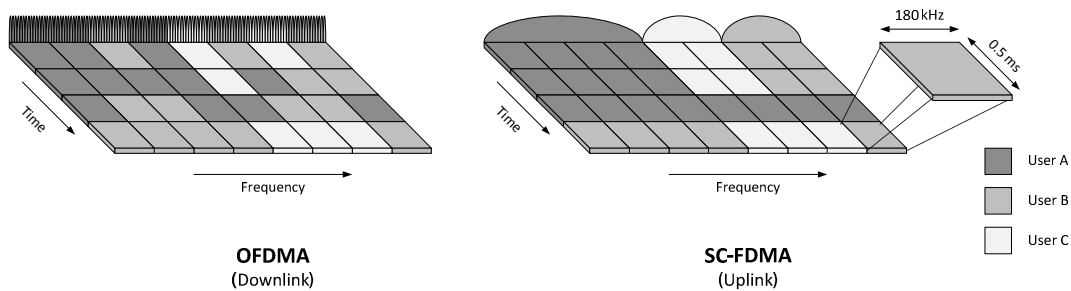

Figure 14 - Time-Frequency structure [17]

3.2.1. Design

OFDMA is distinguished from OFDM in small details. The major advantage of OFDMA regarding OFDM is its scalability of carriers, i.e., OFDMA can allocate a certain number of subcarriers for each user (FDM) and can use all carriers available whenever it needs. Through the TDM (Time Division Multiplexing) technique is assigning a variable time slot to each user to share resources of bandwidth. All these processes are managed by the scheduler.

Nor can we fail to mention that OFDMA presents the same resistance to the damaging effects of multipath delay spread (fading) in the radio channel than OFDM. Without multipath protection, the symbols in the received signal can overlap in time, leading to inter-symbol interference (ISI). OFDMA systems are designed to use in multipath environments, ISI is avoided by inserting a guard period, known as the cyclic prefix (CP), between each transmitted data symbol. The CP is a copy of the end of the symbol inserted at the beginning. By sampling the received signal at the optimum time, the receiver can avoid all ISI caused by delay spread up to the length of the CP. The CP is chosen to be slightly longer than the longest expected delay spread in the radio channel. For the

cellular LTE system, the standard CP length has been set at 4.69 μs, enabling the system to cope with path delay variations up to about 1.4 km. Longer CP lengths are available for use in larger cells and for specialist multi-cell broadcast applications. This provides protection for up to 10 km delay spread but with a proportional reduction in the achievable data rates. Inserting a CP between every symbol reduces the data handling capacity of the system by the ratio of the CP to the symbol length. For LTE, the symbol length is 66.67 μs, which gives a small but significant 7% loss of capacity when using the standard CP (short CP) [21].

In OFDMA systems, the ideal symbol length is defined by the reciprocal of the subcarrier spacing and is chosen to be long compared to the expected delay spread. LTE has chosen 15 kHz subcarrier spacing, giving 66.67 μs for the symbol length. In a single-carrier system, the symbol length is closely related to the occupied bandwidth. For instance, GSM has 200 kHz channel spacing and a 270.833 ksps symbol rate, giving a 3.69 μs symbol length that is 18 times shorter than that of LTE. In contrast, W-CDMA has 5 MHz channel spacing and a 3.84 Msps symbol rate, producing a 0.26 μs symbol length, 256 times shorter than LTE. It would be impractical to insert a 4.69 μs cycle prefix between such short symbols because capacity would drop by more than half with GSM and by a factor of 20 with W-CDMA. Systems that use short symbol lengths compared to the delay spread must rely on receiver-side channel equalizers to recover the original signal. So, the link between channel bandwidth and symbol length puts single-carrier systems at a disadvantage versus OFDMA when the channel bandwidths get wider. Consider a radio channel with 1 μs of delay spread, a 5 MHz single-carrier signal would experience approximately five symbols of ISI and a 20 MHz signal would experience approximately 20 symbols of ISI. The amount of ISI determines how hard the equalizer has to work and there exists a practical upper limit of about 5 MHz beyond which equalizer costs rise and performance drops off.

Long Term Evolution is capable of transmitting 15 ksps in each 15 kHz subcarrier, giving to LTE a raw symbol rate of 18 Msps at its 20 MHz system bandwidth (1200 subcarriers). Using 64QAM, the most complex of the LTE modulation formats, in which one symbol represents six bits, the raw capacity is 108 Mbps ($1200 \times 15000 \times 6 = 108\ Mbps$) to downlink. Note that actual peak rates are derived by subtracting coding and control overheads and adding gains from features such as spatial multiplexing. This is the reason because 108 Mbps does not match the useful bandwidth.

Other advantage over single-carrier systems is the ease with which it can adapt to frequency and phase distortions in the received signal, whether caused by transmitter impairments or radio-channel imperfections. Transmitted and received signals are represented in the frequency domain by subcarrier phase and amplitude. By seeding the transmitted signal across the frequency domain with many reference signals of predetermined amplitude and phase, the receiver can easily correct for frequency-dependent signal distortions prior to demodulation. This correction is particularly necessary when using higher-order modulation formats (e.g. 16QAM, 64QAM) that are susceptible to erroneous symbol demodulation caused by even small errors in phase and amplitude. This ability to easily manipulate phase and frequency also lends itself to the processing

required for MIMO antenna techniques such as spatial multiplexing and beam forming. The required manipulations of signal phase and amplitude are much easier to implement in OFDMA systems than in single-carrier systems, which represent signals in the time domain.

In conclusion, OFDMA is based on OFDM technology. The differences are present in the way resources are shared for bandwidth by multiple users and small details of the OFDM numerology.

3.2.2. Disadvantages

OFDMA has two big disadvantages when compared to single-carrier systems. First, as the number of subcarriers increases, the composite time-domain signal starts to look like Gaussian noise, which has a high peak-to-average power ratio (PAPR) that can cause problems for amplifiers. Allowing the peaks to distort is unacceptable because this causes spectral re-growth in the adjacent channels. Modifying an amplifier to avoid distortion often requires increases in cost, size and power consumption. There exist techniques to limit the peaks (e.g. clipping and tone reservation[6]) but all have limits and can consume significant processing power while degrading in-channel signal quality. Other disadvantage, already cited but very important, is caused by tight spacing of subcarriers, with the goal to minimize the lost efficiency caused by inserting the CP, it is desirable to have very long symbols, which mean closely spaced subcarriers; however, apart from increasing the required processing, close subcarrier restart to lose their orthogonality (independence from each other) due to frequency errors.

The following section presents the alternative specified for LTE UL, since OFDMA does not meet the requisites of the uplink.

3.3. Single-Carrier Frequency Division Multiple Access

The OFDMA signal consists of many subcarriers, where each one is optionally modulated with a high-order modulation scheme (e.g. 64 QAM). The signal, consisting of a high-order modulation combined with a large number of subcarriers, results in a high peak-to-average power ratio (PAPR). This high-order modulation scheme requires very accurate transmit signal generation. The high level of accuracy obliges the OFDMA radio frequency (RF) chain, specifically the power amplifier, to work out its linear zone, trading efficiency for accuracy [26].

---

[6] Tone reservation is an advanced form of clipping in which the time-domain signal is shaped such that the error energy falls on specific, reserved in-channel frequencies, ensuring less distortion in the wanted part of the signal.

LTE uplink requirements differ from downlink requirements in several ways. OFDMA is considered power inefficient, however, it is tolerable in the case of DL transmission because the power amplifier is placed at the base station (eNodeB in 3GPP terminology). In the base-station, power is available and the extra complexity is shared over many mobile terminals. On the other hand, most of the mobile terminals are battery powered, and constrained to be of low cost to enable mass deployment. Thereby, the undesirable high PAPR of OFDMA led 3GPP to choose a different modulation format for the LTE UL. 3GPP specifications suggested a new hybrid modulation scheme that cleverly combines the low PAPR of single-carrier systems with robust resistance to multipath and flexible subcarrier frequency allocation offered by OFDMA called SC-FDMA. This eases the mobile terminal task of maintaining highly efficient signal transmission by its power amplifier, achieving this property without degradation in the system flexibility and performance.

The use of SC-FDMA in LTE, however, is restricted to the uplink because a drawback observed for the SC-FDMA is an increase in complexity of both the receiver and transmitter. While the additional complexity added to the transmitter is considered as negligible, the increase in complexity of the receiver is larger considering the requirement of supporting multiple users in parallel [2].

In this section is described the whole structure of an SC-FDMA system, however it will be avoided the formal mathematical approach, unlike will be preferred several graphical comparisons of the differences between OFDMA and SC-FDMA. For a formal definition of SC-FDMA, it is needed look no further than [3], which gives the mathematical description of the time-domain representation of an SC-FDMA symbol.

3.3.1. Design

The uplink uses the same generic frame structure as the downlink, see Figure 9, as also uses the same subcarrier spacing of 15 kHz and PRB width (12 subcarriers). Downlink modulation parameters (including short and long CP length) are identical to the uplink parameters shown in Table 2. Not surprisingly, subcarrier modulation is, however, much different. Power consumption is a key consideration for UE terminals.

The basic transmitter and receiver SC-FDMA architecture is very similar (nearly identical) to OFDMA, since that re-uses many OFDMA functional blocks. Thus, there is a significant degree of functional commonality between the uplink and downlink signal chains. Multipath distortion is also handled in the same manner as in OFDMA systems (removal of CP, conversion to the frequency domain, then apply the channel correction on a subcarrier-by-subcarrier basis). Presenting the same degree of multipath protection with lower PAPR (by approximately 2 dB) due

to the underlying waveform is essentially single-carrier. Figure 15 shows the diagram of a basic SC-FDMA transmitter and receiver arrangement [26].
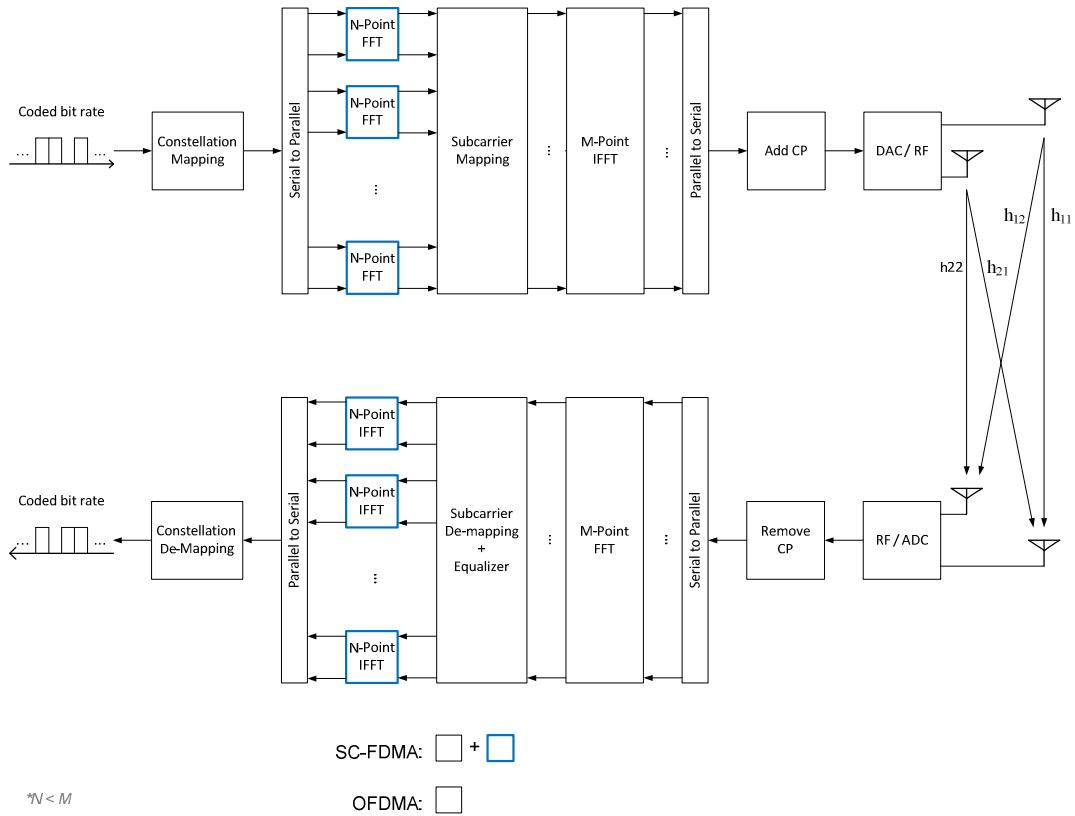

Figure 15 - Adjacent transmitter and receiver structure of the proposed UL SC-FDMA scheme

The functional blocks in the transmit chain are:

- **Constellation mapping:** Converts incoming bit stream to single carrier symbols (BPSK, QPSK, or 16QAM depending on channel conditions) and injects them into the serial to parallel converter;

- **Serial/parallel converter**: Formats time domain SC symbols into blocks for input to FFT engine;

- **N-point DFT**: Converts time domain SC symbol block into N discrete tones;

- **Subcarrier mapping**: Maps DFT output tones to specified subcarriers for transmission. SC-FDMA systems either use contiguous tones (adjacent) or uniformly spaced tones

(distributed). The trades between adjacent and distributed subcarrier mapping are discussed further below;

- **M-point IDFT**: Converts mapped subcarriers back into time domain for transmission;

- **Cyclic prefix**: Cyclic prefix is prepended to the composite SC-FDMA symbol to provide multipath immunity in the same manner as described for OFDM;

- **DAC/RF**: Converts digital signal to analog and up convert to radio frequency (RF) for transmission.

The input to the block diagram is a stream of bits, which are modeled onto a signal constellation points that can be BPSK, QPSK or 16QAM depending on channel quality (i.e., complex numbers representing symbols). However, rather than using symbols to directly modulate subcarriers (as is the case in OFDMA), uplink symbols are sequentially fed into a serial/parallel converter and then into an FFT module of N_{TX} points, as shown in Figure 15. This module is particular to SC-FDMA and it may be viewed as a pre-process to the large size IFFT. The result at the output of the FFT block is a discrete frequency domain representation of the symbol sequence. From the Subcarrier Mapping stage and onwards, the signal flow is similar to a conventional OFDMA modulator, i.e. the discrete Fourier terms at the output of the FFT block are then mapped to subcarriers before being converted back into the time domain (IFFT). The IFFT module output is followed by a cyclic prefix insertion that completes the digital stage of the signal flow. The final stage in the flow converts the digital signal to an analog signal and up convert to radio frequency (RF) for transmission. It is interesting to note that while the SC-FDMA signal has a lower PAPR in the time domain, individual subcarrier amplitudes can actually vary more in the frequency domain than a comparable OFDM signal [24].

In the receive side chain, the process is essentially reversed. However, the receiver structure has an additional conventional functionality, such as channel-estimation and equalization. The receiver diagram assumes perfect timing and frequency synchronization for the sake of simplicity.

As stated, the Subcarrier Mapping block controls the frequency allocation, however there are two principal modes of frequency resource allocation in 3GPP-LTE UL: adjacent allocation (A-FDMA) and distributed allocation (D-FDMA) [24][26]. A-FDMA is considered simpler to signal in terms of control signaling overhead. On the other hand, it suffers from a low level of frequency diversity. To gain frequency diversity, it is proposed to use a distributed scheme (D-FDMA). In this scheme the DFT stage output is evenly distributed over the entire (or a part of the entire) symbol BW, which is larger than the original signal BW. A special case of D-FDMA, in which the transmission occupies the entire BW, is usually termed as interleaved FDMA (I-FDMA).

It should be observed that the DFT followed by IFFT in an A-FDMA setup operates as an efficient implementation to an interpolation filter. This may justify the reduced PAPR experienced in the

IFFT output; the signal remains in the symbol constellation space. A similar observation holds also for the D-FDMA and I-FDMA.

Figure 16 illustrates the two modes of operation. The left hand side of Figure 2 presents a adjacent allocation where the transmitted signal occupies N_{TX} consecutive subcarriers. The right hand side of the figure presents a distributed allocation where N_{TX} inputs are evenly separated.
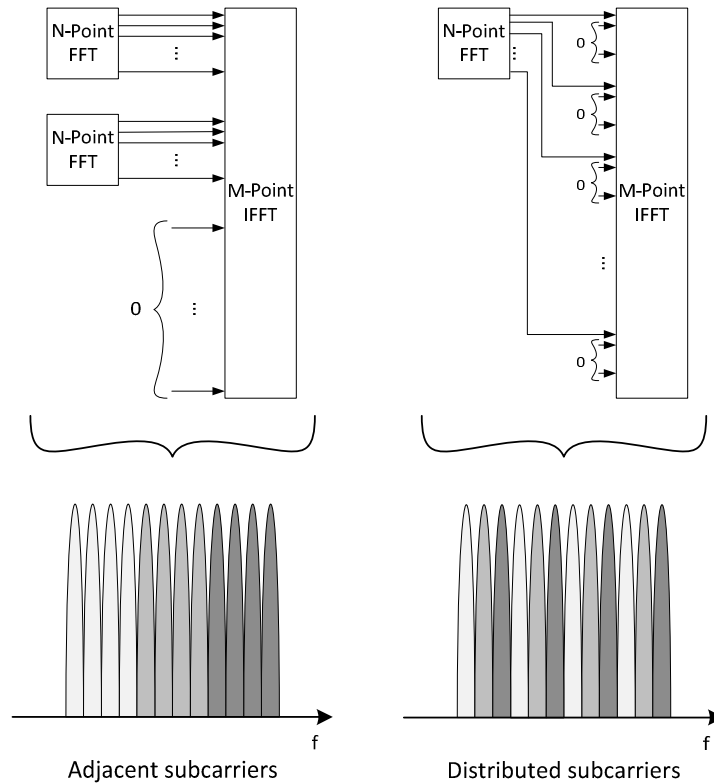

Figure 16 - SC-FDMA Subcarriers can be mapped in either adjacent or distributed mode

Adjacent mapping is characterized by low frequency diversity, higher BER and FER for narrowband users, time domain channel has larger power fluctuations, difficult to choose appropriate modulation and coding scheme due to rapid channel fluctuations and less accurate power control, low-rate user may block a high-rate (broadband) user from the channel, especially if channel dependent scheduling is used and channel estimation not degraded at low bandwidths.

Interleaved mapping is characterized by larger frequency diversity, low-rate and high-rate users coexist peacefully, time domain channel has less power fluctuation, more stable modulation and coding control, more accurate power control, channel estimation becomes degraded for very large repetition factors and tighter frequency synchronization may be required.

Chapter 4

4. MIMO spatial multiplexing

Applying multiple antennas at both ends of a communication system can not only greatly improve the capacity and the throughput of a wireless link in flat fading but also in frequency selective fading channels, especially when the environment provides rich scattering.

Multiple Input Multiple Output systems, also known as MIMO, have multi-element antenna arrays at both transmit and receive sides. High data rates are achieved when implementing such structures without increasing, neither the bandwidth nor the total transmission power. Additionally, the use of multiple antennas at both transmitter and receiver provides a diversity advantage, i.e. improvement in SNR and hence in BER at the receiver [27] [28].

This chapter begins with an introductory section where we introduce MIMO schemes and diversity gain. Then, we describe and develop a mathematical framework to model MIMO systems. Here we present the Alamouti concept.

4.1. MIMO communications

When communicating through a wireless channel, transmitted signals suffer from attenuation and fading due to multipath in the channel, thus making it difficult for the receiver to determine these signals. Diversity techniques take advantage of the multipath propagation characteristics to improve receiver sensitivity. MIMO systems utilize antenna diversity to obtain the mentioned improvement and hence combat fading.

A MIMO system characterizes itself by using multiple antennas at both transmitter and receiver. However, if only multiple antennas are deployed at one end of the communication system, or both ends use a single antenna, the MIMO system changes into a SIMO, MISO or SISO system [29], as shown in Figure 17. In this way, when only multiple antennas are deployed at the receiver, the MIMO system reduces to a Single Input Multiple Output (SIMO) system. Similarly, when the system has only one receive antenna but multiple antennas at the transmitter side, the MIMO system reduces to a Multiple Input Single Output (MISO). Finally, when both, transmitter and receiver, use a single antenna, the MIMO system simplifies to a Single Input Single Output (SISO) system.
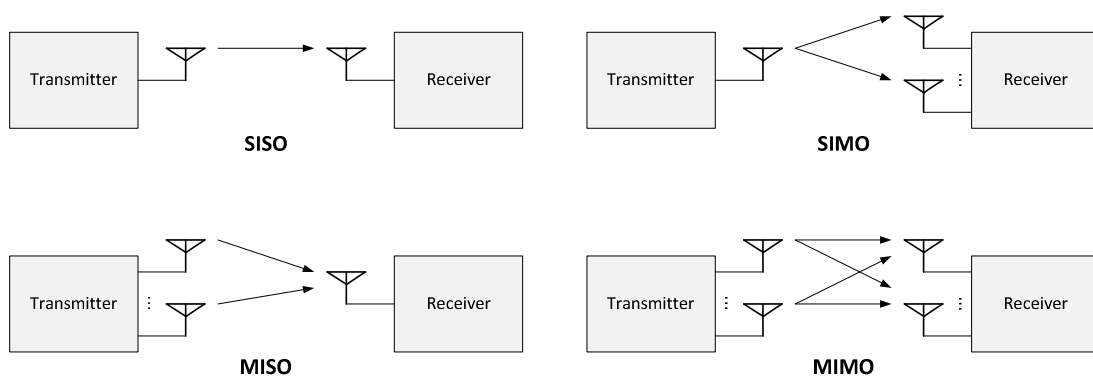
Figure 17 - MIMO schemes

The main advantages of MIMO channels over traditional SISO channels are the array gain, the diversity gain, and the multiplexing gain. Array gain and diversity gain are not exclusive of MIMO channels and also exist in SIMO and MISO channels. Multiplexing gain, however, is a unique characteristic of MIMO channels [30]. Array gain is the improvement in SINR[7] obtained by coherently combining the signals on multiple transmits or multiple receive dimensions and is easily characterized as a shift of the BER curve due to the gain in SINR. Diversity gain is the improvement in link reliability obtained by receiving replicas of the information signal through independently fading links, branches, or dimensions. It is characterized by a steepen slope of the BER curve in the low BER region or high SNR regime.

The three major forms of diversity exploited in wireless communication systems are temporal, frequency, and spatial diversity. Transmit diversity is more difficult to exploit than receive diversity since special modulation and coding schemes are required, i.e. space-time coding, whereas receive diversity simply needs the multiple receive dimensions to fade independently without requiring any specific modulation or coding scheme.

4.1.1. The MIMO channel model

Assuming flat fading channels, the signal model for a MIMO channel composed by N_T transmitting and N_R receiving dimensions is

$$\boldsymbol{y} = \boldsymbol{Hs} + n \tag{4.1}$$

---

[7] Signal to Interference-plus-Noise Ratio is defined as the ratio of signal power to the combined noise and interference power.

where $s \in \mathbb{C}^{N_T \times 1}$ is the transmitted data vector, $H \in \mathbb{C}^{N_R \times N_T}$ is the channel matrix, $y \in \mathbb{C}^{N_R \times 1}$ is the received vector, and $n \in \mathbb{C}^{N_R \times 1}$ is the noise vector. This signal model represents a single transmission. Figure 18 depicts a MIMO scenario with N_T transmit antennas and N_R receive antennas. The signals at the transmit antenna array are denoted by vector $s = \left[s_1, \ s_2, \cdots , \ s_{N_T}\right]^T$, and similarly, the signals at the receiver are $y = \left[y_1, \ y_2, \cdots , \ y_{N_R}\right]^T$, where $(\cdot)^T$ denotes transposition, and s_m and y_m are the signals at the $m\text{-}th$ transmit antenna port and at the $m\text{-}th$ receive antenna port, respectively.
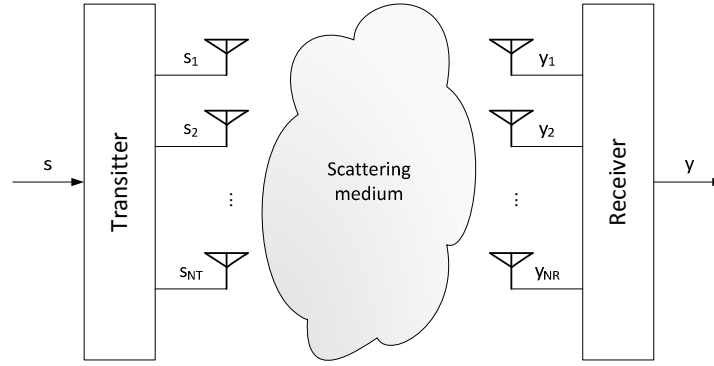

Figure 18 - A MIMO channel model in a scattering environment.

The MIMO radio channel describing the connection between transmitter and receiver can be expressed as

$$H = \begin{pmatrix} \alpha_{11} & \alpha_{12} & \cdots & \alpha_{1N_T} \\ \alpha_{21} & \alpha_{22} & \cdots & \alpha_{2N_T} \\ \vdots & \vdots & \ddots & \vdots \\ \alpha_{N_R 1} & \alpha_{N_R 2} & \cdots & \alpha_{N_R N_T} \end{pmatrix} \tag{4.2}$$

where α_{nm} is the complex transmission coefficient from antenna m at the transmitter to antenna n at the receiver. Moreover, the path gains $\{\alpha_{ij}\}$, are correlated depending on the propagation environment, the polarization of the antenna elements, and the spacing between them.

4.2. Space-Time Coding

Space-time coding (STC) is an efficient approach to exploit the enormous diversity offered by the MIMO. It is used to obtain gains due to spatial diversity via multiple transmit and receive antennas. Moreover, a diversity gain proportional to the number of antennas at both transmit and receive sides can be achieved. One popular representation of these codes is the Alamouti scheme [31] for two transmit antennas.

STC techniques are used to improve the performance of MIMO systems. Their central issue is the exploitation of multipath effects in order to achieve very high spectral efficiency. With this purpose, the principal aim of the space-time coding lies in the design of two-dimensional signal matrices to be transmitted during a specified time period on a number of antennas. Thus, it introduces redundancy in space through the addition of multiple antennas, and redundancy in time through channel coding, enabling us to exploit diversity in the spatial dimension, as well as a obtaining a coding gain. Therefore, the transmit diversity plays an integral role in the STC design.

4.2.1. The Alamouti concept

Alamouti [31] [32] introduced a very simple scheme of space-time block coding (STBC) allowing transmissions from two antennas with the same data rate as on a single antenna, but increasing the diversity at the receiver from one to two in a flat-fading channel. As shown in Figure 19, the Alamouti algorithm uses the space and the time domain to encode data, increasing the performance of the system by coding the signals over the different transmitter branches. Thus, the Alamouti code achieves diversity two with full data rate as it transmits two symbols in two time intervals.
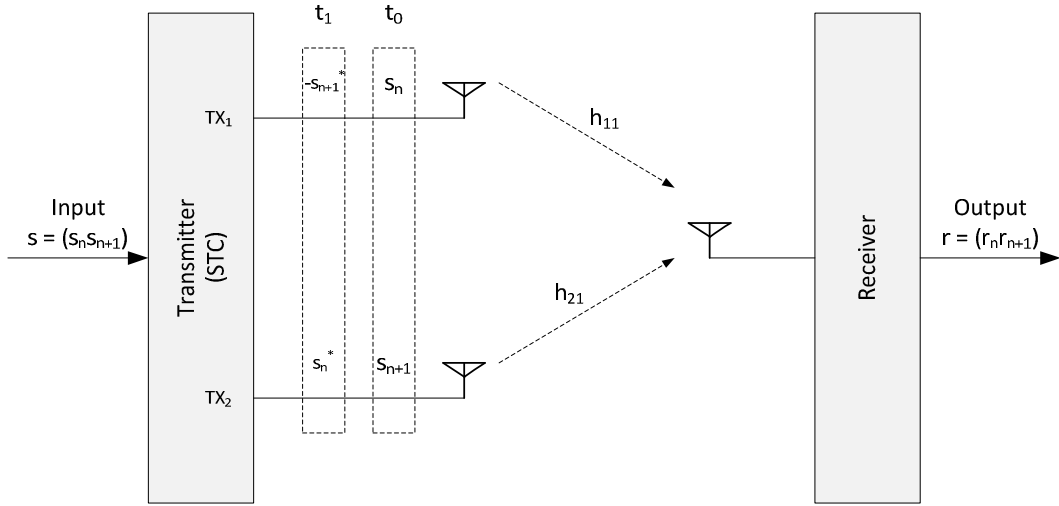
Figure 19 - 2×1 Alamouti scheme.

In the first time slot, transmit antennas TX_1 and TX_2 are sending symbols s_n and s_{n+1}, respectively. In the next time slot, symbols $-s_{n+1}^*$ and s_n^* are sent, where $(\cdot)^*$ denotes complex conjugation. Each symbol is multiplied by a factor of a squared root of two in order to achieve a transmitted average power of one in each time step. Furthermore, it is supposed that the channel, which has transmission coefficients, h_{11} and h_{12}, remains constant and frequency flat over the two consecutive time steps.

The received vector, **r**, is formed by stacking two consecutive received data samples in time, resulting in

$$r = \frac{1}{\sqrt{2}} . S . h + n \tag{4.3}$$

where $r = [r_n, r_{n+1}]^T$ represents the received vector, h_1 represents the channel between the antenna TX_1 and receiving antenna, h_2 represents the channel between the antenna TX_2 and the same receiving antenna, i.e. $h = [h_{11}, h_{12}]^T$ is the complex channel vector, $n = [n_0, n_1]^T$ is the noise at the receiver, and **S** defines the STC:

$$S = \begin{pmatrix} s_n & s_{n+1} \\ s_{n+1}^* & -s_n^* \end{pmatrix} \tag{4.4}$$

The vector equation in Equation 4.3 can be read explicitly as

$$r_n = \frac{1}{\sqrt{2}} s_n h_{11} + \frac{1}{\sqrt{2}} s_{n+1} h_{12} + n_0 \tag{4.5}$$

$$r_{n+1} = \frac{-1}{\sqrt{2}} s_{n+1}^* h_{11} + \frac{1}{\sqrt{2}} s_n^* h_{12} + n_1 \tag{4.6}$$

41

At the receiver, the vector y of the received signal is formed according to $\boldsymbol{y} = [r_0, r_1^*]^T$, which is equivalent to

$$r_n = \frac{1}{\sqrt{2}} s_n h_{11} + \frac{1}{\sqrt{2}} s_{n+1} h_{12} + n_0 \tag{4.7}$$

$$r_{n+1}^* = \frac{1}{\sqrt{2}} s_n h_{12}^* - \frac{1}{\sqrt{2}} s_{n+1} h_{11}^* + n_1^* \tag{4.8}$$

These both equations can be rewritten in a matrix system as specified in Equation 4.9:

$$\begin{pmatrix} r_n \\ r_{n+1}^* \end{pmatrix} = \frac{1}{\sqrt{2}} \begin{pmatrix} h_{11} & h_{12} \\ h_{12}^* & -h_{11}^* \end{pmatrix} \begin{pmatrix} s_n \\ s_{n+1} \end{pmatrix} + \begin{pmatrix} n_0 \\ n_1^* \end{pmatrix} \tag{4.9}$$

The short notation for this system is the following

$$\boldsymbol{y} = \frac{1}{\sqrt{2}} \boldsymbol{H}_v \boldsymbol{s} + \tilde{\boldsymbol{n}} \tag{4.10}$$

where $\tilde{\boldsymbol{n}}$ represents the new noise vector obtained after the conjugation of the second equation, $\tilde{\boldsymbol{\eta}} = [n_0, n_1^*]^T$.

The resulting virtual (2 × 2) channel matrix, $\boldsymbol{H}_v$, is orthogonal, i.e.

$$\boldsymbol{H}_v{}^H \boldsymbol{H}_v = \boldsymbol{H}_v \boldsymbol{H}_v{}^H = h^2 \boldsymbol{I}_2 \tag{4.11}$$

where $(\cdot)^H$ represents the hermitian operation, $\boldsymbol{I}_2$ is the 2×2 identity matrix, and h^2 is the power gain of the channel, with $h^2 = |h_{11}|^2 + |h_{12}|^2$. Due to this orthogonality, the Alamouti scheme decouples the MISO channel into two virtually independent channels with channel gain h^2 and diversity $d = 2$.

The mentioned channel gain is deduced from Equation 4.12, which specifies that transmitted symbols can be estimated at the receiver as the result of multiplying the received signals by the hermitian of the virtual channel matrix. After performing the corresponding operations it results in a signal with a gain of h^2 plus some modified noise.

$$\hat{\boldsymbol{s}} = \boldsymbol{H}_v{}^H \boldsymbol{y} = \frac{1}{\sqrt{2}} h^2 \boldsymbol{s} + \boldsymbol{H}_v{}^H \tilde{\boldsymbol{n}} \tag{4.12}$$

4.2.2. Alamouti scheme with arbitrary number of receive antennas

A system with two transmit antennas and an arbitrary number of receive antennas [33], as the one depicted in Figure 20, is analyzed next. The already explained steps are applied to each of the receive antennas, denoting the received signal in the first and second time slot as r_0 and r_1, respectively.
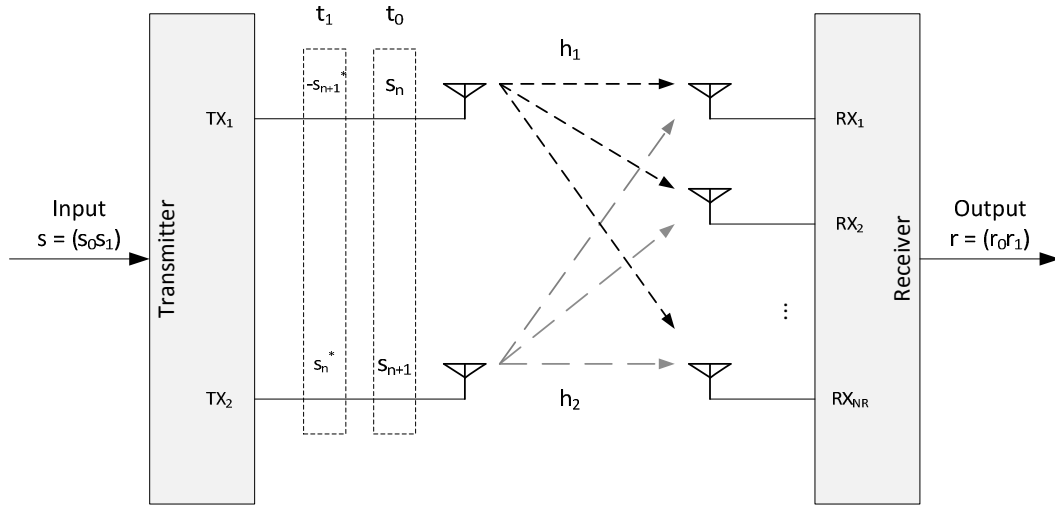

Figure 20 - 2×NR Alamouti scheme

Vectors $\boldsymbol{h}_1 = \left[h_{11}, \ h_{12}, \cdots, \ h_{1N_R}\right]^T$ and $\boldsymbol{h}_2 = \left[h_{21}, \ h_{22}, \cdots, \ h_{2N_R}\right]^T$ contain the channel coefficients corresponding to the transmission from antenna TX_1 and antenna TX_2 to every receive antenna, respectively.

As in the previous section, the received vector is

$$\begin{pmatrix} y_n \\ y_{n+1} \end{pmatrix} = \begin{pmatrix} r_n \\ r_{n+1}^* \end{pmatrix} = \frac{1}{\sqrt{2}} \begin{pmatrix} h_1 & h_2 \\ h_2^* & -h_1^* \end{pmatrix} \begin{pmatrix} s_n \\ s_{n+1} \end{pmatrix} + \begin{pmatrix} n_0 \\ n_1^* \end{pmatrix}$$ (4.13)

where n_0 and n_1 are noise vectors, corresponding to the noise added in each receive branch.

Following the same steps as in the 2×1 Alamouti scheme, the estimation of the transmitted symbols at the receiver is performed in Equation 4.14. Since the power gain of the channel is, in this case, $h^2 = \|\boldsymbol{h}_1\|^2 + \|\boldsymbol{h}_2\|^2$, it is possible to achieve a diversity order of $2N_R$.

$$\hat{\boldsymbol{s}} = {\boldsymbol{H}_v}^H \boldsymbol{y} = \frac{1}{\sqrt{2}} h^2 \boldsymbol{s} + {\boldsymbol{H}_v}^H \tilde{\boldsymbol{n}}$$ (4.14)

For a system with two receive antennas, RX_1 and RX_2, and according to the above equations, the received signals would be $\boldsymbol{r}_n = [r_n(1), r_n(2)]^T$ and $\boldsymbol{r}_{n+1} = [r_{n+1}(1), r_{n+1}(2)]^T$, where $r_n(1)$ is the symbol received in antenna RX_1 at time slot t_0, and $r_{n+1}(1)$, the symbol received at time slot t_1. In the same way, $r_n(2)$ and $r_{n+1}(2)$ are the symbols received in antenna RX_2 during the two time slots. Therefore, the signal that is received at the end is $\boldsymbol{y} = [r_n, r_{n+1}^*]^T$:

$$
\begin{pmatrix} r_n \\ r_{n+1}^* \end{pmatrix} = \begin{pmatrix} r_n(1) \\ r_n(2) \\ r_{n+1}^*(1) \\ r_{n+1}^*(2) \end{pmatrix} = \frac{1}{\sqrt{2}} \begin{pmatrix} h_{11} & h_{21} \\ h_{12} & h_{22} \\ h_{21}^* & -h_{11}^* \\ h_{22}^* & -h_{12}^* \end{pmatrix} \begin{pmatrix} s_n \\ s_{n+1} \end{pmatrix} + \begin{pmatrix} \eta_0(1) \\ \eta_0(2) \\ \eta_1^*(1) \\ \eta_1^*(2) \end{pmatrix}
\tag{4.15}
$$

In this case the power gain of the channel is $h^2 = \|\boldsymbol{h}_1\|_2^2 + \|\boldsymbol{h}_2\|_2^2$ and a diversity order of 4 is achieved.

Chapter 5

5. LTE Uplink Simulation

Throughout this dissertation we have been introducing the main theoretical concepts of physical layer of LTE. In this chapter we report the entire implementation and validation work. We begin with a comprehensive description of the models implemented over the simulation platform used to simulate the uplink of LTE (SC-FDMA), in Section 5.1; Then, we describe the algorithms and mathematical models used to understand how the different equalizers improve data reception for different antennas schemes, in Section 5.2; and finally we analyzed the results of various scenarios in Section 5.3. All conclusions will be underpinned by practical results.

5.1. Simulation platform of the SC-FDMA

In this section we describe the SC-FDMA based system implemented. All the main theoretical background was explained in chapters 3 and 4, where we introduce the SC-FDMA structure and MIMO diversity, respectively.

Figure 21 shows the implemented platform. It comprises several blocks:

- **Channels Generation's block** is responsible for generating the matrices that emulate the channel's effect in frequency-domain to several users, i.e. the effect suffered by the radio signal when it is propagated through a medium wireless corresponding to each channel (H_{11}, H_{12}, H_{21} and H_{22});

- **Data Generation's block** has the simple task to generate arrays of random bits (0 and 1), in accordance with the number of users, the encoder and the modulation used to each simulation;

- **Coder's block**, as own name indicates, is in charge of encoding the data bits generated by the Data Generation's block. Allowing to choose among three mode of operation: without coding, CTC encoder (turbo coding) and CC63 encoder (convolutional coding);

- **Data Modulation's block** converts incoming bit stream to single carrier symbols spatially allocated (digital modulation schemes available: BPSK, QPSK, 16QAM and 64QAM) and injects them SC-FDMA structure;

- **SF Processing's block** formats time-domain symbols into blocks for input to FFT engine that converts time-domain single carrier symbol block into N discrete tones, i.e. performs Fast Fourier Transform with variable size of number of subcarriers. Finally, to emulate the spatial diversity antenna is performed space-time block coding (STBC). However, these schemes require that the channel remains constant over two OFDM transmission periods for Alamouti coding or even more if other codes are employed to achieve good performance. Such condition may be hard to uphold in multicarrier systems and therefore to overcome the time invariance limitation, an alternative is to send the code symbols on different subcarriers. In [34] an efficient implementation of space-frequency block coding (SFBC)is discussed for OFDM;

- **OFDM Framing's blocks** maps DFT output tones to specified subcarriers into SC-FDMA frame for each user, either in contiguous tones (adjacent mapping) or uniformly spaced tones (interleaved mapping). In practical terms to support multiple users, the frame of each user is sent in series because it would be impractical to implement a transmitter for each user, see Figure 22;

- **CFR's blocks** adds the respective channel's effect for each SC-FDMA frame;

- **Add AWGN's block** adds additive white Gaussian noise (AWGN);

- **OFDM De-framing's block** unmaps the frame into a vector taking into account the operation mode (adjacent or interleaved mapping);

- **Equalizer's block** performs space frequency combining (SFC) and applies equalization's algorithms (MMSEC, ZFC, EGC and MRC), aimed at lessening the channel's effect, ISI and noise, and also performs the IFFT with the respective size converting mapped subcarriers back into time-domain;

- **Data Demodulation's block** converts incoming single carrier symbols spatially allocated into bits according to the modulation scheme used;

- **Channel Weighting's block** multiplies the equivalent channel for each bit when data is encoded;

- **Decoder's block** does the reverse process of Coder's block extracting all data;

- **Checker's block** checks if the received bits correspond to the transmitted bits, and accounts error bits, error frames, received bits and runs.
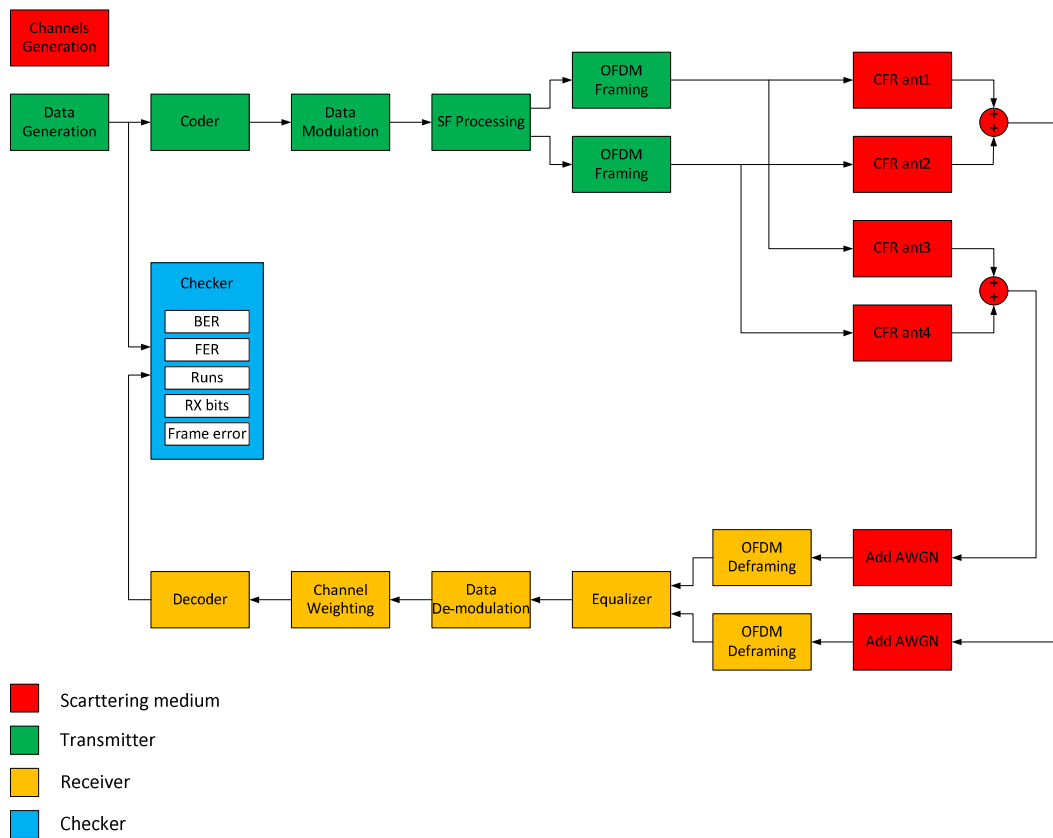
Figure 21 - Simulation platform of the SC-FDMA
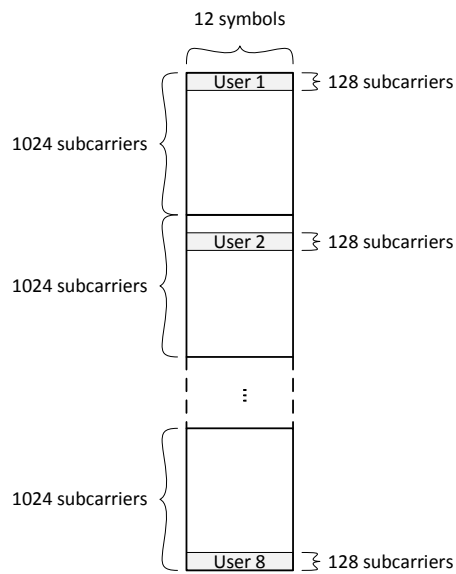
Figure 22 - SC-FDMA frames from all users in series

In parallel, we developed a simulation window, as shown in Figure 23, where we can set all simulation parameters. This window interacts with the platform and automatically activates all requirements necessary for simulation to simulation. This tool comes to facilitate the simulation of scenarios.

Figure 23 - Simulation window

Figure 24 illustrates the block diagram that represents all the functions proposed for the platform, analogous to the SC-FDMA structure presented in Chapter 3, allowing a better understanding about the developed platform.

SC-FDMA Transmitter Sctruture (users)

Bit rate
1 0 0 1 1 1 …

Coded symbol rate

Data Generation → Coder → Constellation Mapping → Add K Users

Users 1, …, K

MAX = 8 users (1536 symbols per user)

Serial to Parallel → N-Point FFT → SFBC → Subcarrier Mapping + Chip interleaver → Antenna 1 → Channel 1 / Channel 3

Subcarrier Mapping + Chip interleaver → Antenna 2 → Channel 2 / Channel 4

Checker: BER / FER / Runs / RX bits / Frame error

SC-FDMA Receptor Sctruture (base station)

Bit rate
… 1 1 1 0 0 1

Coded symbol rate

Decoder → Equalizer Channel Weighting → Constellation De-Mapping → Equalizer → Parallel to Serial → N-Point IFFT → SFC + Equalization → Subcarrier De-Mapping + Chip De-interleaver → Antenna 1 → Add AWGN

Figure 24 - SC-FDMA Architecture

In order to simplify the implementation, it was considered a fixed frame of 1024 subcarriers with a slot of 12 consecutive OFDM symbols. We also consider a constant number of 128 subcarriers per user, corresponding to a maximum of 8 users. In other words, the first three blocks of the diagram (Data Generation, Coder and Data Modulation), must be aligned to ensure that in each runs they're generated 1536 symbols per user, independent of the encoder (CTC and CC63) and modulation (BPSK, QPSK, 16QAM and 64QAM). Table 4 displays all the configurable parameters featuring all the scenarios.

Table 4 - Configurable Parameters

Modulation	BPSK or QPSK or 16QAM or 64 QAM
Number of users	1 – 8 (full load)
Number of FFT tones	16 or 32 or 64 or 128
Channel profile	AWGN or ITU pedestrian channel model B
Channel coder	Off or CTC or CC63
Interleaver processing	On or Off
Equalizer's algorithms	MRC or EGC or ZFC or MMSEC
MIMO schemes	1×1 or 1×2 or 2×2

5.2. Mathematical analysis

In this section we derive the expressions of the several multiple antennas techniques characteristic of the LTE UL: SISO, SIMO and MIMO. As also we present all the equalizers considered in this work.

5.2.1. SISO

Let's start with the simplest system, where both terminals are equipped with single antenna, as shown in Figure 25.
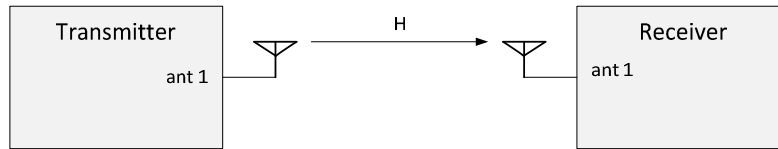

Figure 25 - SISO scheme (1×1)

Considering a row vector of L symbols, $\boldsymbol{d} = [d_1, \dots, d_L]$, the transmitted signal in the frequency-domain, $\boldsymbol{s}$, is given by

$$\underset{1 \times L}{\boldsymbol{s}} = \underset{1 \times L}{\boldsymbol{d}} \cdot \underset{L \times L}{\boldsymbol{F}} \tag{5.1}$$

where $\boldsymbol{F}$ represents the square matrix $L \times L$ of the Discrete Fourier Transform (DFT).

Posteriorly, the received signal, $\boldsymbol{y}$, is given by

$$\underset{1 \times L}{\boldsymbol{y}} = \underset{1 \times L}{\boldsymbol{s}} \cdot \underset{L \times L}{\boldsymbol{H}} + \underset{1 \times L}{\boldsymbol{n}} \tag{5.2}$$

where $\boldsymbol{H}$ represents the square matrix $L \times L$ of the complex flat-fading channels coefficients over L subcarriers, and $\boldsymbol{n}$ means the additive white Gaussian noise (AWGN), with zero mean and variance σ^2.

After replacing equation 5.1 in 5.2, we can write

$$\underset{1 \times L}{\boldsymbol{y}} = \underset{1 \times L}{\boldsymbol{d}} \cdot \underset{L \times L}{\underbrace{\boldsymbol{F}.\boldsymbol{H}}} + \underset{1 \times L}{\boldsymbol{n}} \tag{5.3}$$

Upon receipt the signal is necessary estimate the transmitted symbols, which requires channel equalization, i.e., we need to remove or minimize the channel's effect and the noise. Therefore, the estimated symbols, $\widehat{d}$, after the IFFT operation are given by

$$\underset{1\times L}{\widehat{\pmb{d}}} = \underset{1\times L}{\underline{\pmb{y}}} \cdot \underset{L\times L}{\underline{\pmb{G}.\pmb{F}^H}} \tag{5.4}$$

where $\pmb{G}$ and $\pmb{F}^H$ represents the square matrix $L \times L$ of the equalizer coefficients and the inverse Discrete Fourier Transform coefficients (IDFT), respectively. Note that $\pmb{F}.\pmb{F}^H = \pmb{I}_L$, where $\pmb{I}_L$ represents the identity matrix of size $L \times L$.

Replacing equations 5.3 in 5.4, we can write

$$\underset{1\times L}{\widehat{\pmb{d}}} = \underset{1\times L}{\underline{\pmb{d}}} \cdot \underset{L\times L}{\underline{\pmb{F}.\pmb{H}.\pmb{G}.\pmb{F}^H}} + \underset{1\times L}{\underline{\pmb{n}}} \cdot \underset{L\times L}{\underline{\pmb{G}.\pmb{F}^H}} \tag{5.5}$$

From equation 5.5 we can conclude that the data symbol vector is perfectly estimated at the receiver if $\pmb{F}.\pmb{H}.\pmb{G}.\pmb{F}^H = \pmb{I}$, i.e., only if the effects of the channel are full eliminated, otherwise a given data symbol suffer from interference of others. Thus, the equalizer plays an important role on the system performance.

So, the soft estimation of a generic data symbol j is given by

$$\widehat{\pmb{d}}_j = \underset{Desired\ Signal}{\underline{\pmb{d}_j.\pmb{f}_j.\pmb{H}.\pmb{G}.\pmb{f}_j^H}} + \underset{ISI}{\underline{\sum_{k=1,\ k\neq j}^{K} \pmb{d}_k.\pmb{f}_k.\pmb{H}.\pmb{G}.\pmb{f}_j^H}} + \underset{Noise}{\underline{\pmb{n}.\pmb{G}.\pmb{f}_j^H}} \tag{5.6}$$

where $\pmb{f}_j$ represents the $j\text{-}th$ row of matrix $\pmb{F}$. It is clear that the equalizer is intended to reduce the effect of ISI and noise. Ideally, the negative effects of ISI and Gaussian noise are completely cancelled by the equalizer. However, no equalizer presents an ideal behaviour. In conclusion, the received signal consists by the desired signal, inter-symbols interference and noise. The purpose of the equalizer is to minimize the effect of the last two.

In the SC-FDMA systems can be used four different types of single user equalizers: Maximum Ratio Combine (MRC), Equal Gain Combining (EGC), Zero Forcing Combining (ZFC) and Minimum Mean Square Error Combining (MMSEC). The equalization coefficients are defined as $g_{j,n}^{(i)}$, where i is the $i\text{-}th$ transmit antenna, j is the $j\text{-}th$ data symbol and n is the $n\text{-}th$ subcarrier equalization.

1. Maximum Ratio Combining

MRC equalization aims to maximize the instantaneous SNR at the receiver's front end. The equalizer coefficients are obtained simply from the complex conjugate of the frequency response of the channel. Under the MRC criterion, the equalization weights are

$$g_{j,n}^{(i)} = h_{j,n}^*$$
(5.7)

2. Equal Gain Combining

In order to arrive all the subcarriers at the receiver in phase, phase equalization can be performed at the transmitter in the form of EGC. This scheme compensates only the phase rotation caused by the channel. Under the EGC criterion, the coefficients are given by

$$g_{j,n}^{(i)} = \frac{h_{j,n}^*}{|h_{j,n}|}$$
(5.8)

This technique is less complex, since it only requires the phase information of the channel coefficients. What makes it particularly interesting in the DL, since the mobile only needs estimate the phase of the channel.

3. Zero Forcing Combining

The equalizer constructed under the ZFC criterion represents the inverse of the channel's frequency response. For the i-th transmit antenna and the j-th data symbol, the equalizer coefficients are obtained using the ZFC, simply flipping the channel

$$g_{j,n}^{(i)} = \frac{h_{j,n}^*}{|h_{j,n}|^2}$$
(5.9)

This scheme restores the orthogonality among different users, forcing the ISI to zero. However, a major drawback of this scheme is that it amplifies noise especially for the channel coefficients with low amplitude.

4. Minimum Mean Square Error Combining

In this scheme, the coefficients are obtained by minimizing the mean squared error between the transmitted signal before OFDM modulation and signal to the equalizer on each subcarrier.

$$g_{j,n}^{(i)} = \frac{h_{j,n}^*}{|h_{j,n}|^2 + \sigma^2}$$
(5.10)

It is easy to verify that to $\sigma^2 \to \infty$ the MMSE equalizer is identical to the ZFC. As we shall see in section 5.3, this equalization algorithm will be that which it presents the best results.

5.2.2. SIMO

The second scenario is the SIMO scheme with an antenna on the side of the transmitter and two antennas at the receiver, as shown in Figure 26.
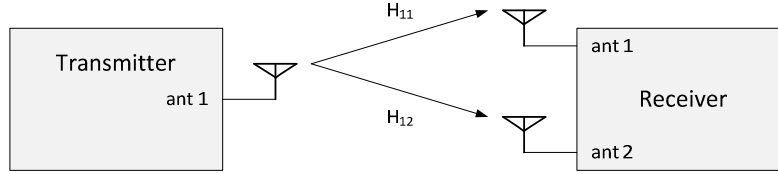

Figure 26 - SIMO scheme (1×2)

Once again considering a row vector of L symbols, $\boldsymbol{d} = [d_1, \ldots, d_L]$, the transmitted signal in the frequency-domain, $\boldsymbol{s}$, is given by

$$\underset{1 \times L}{\boldsymbol{s}} = \underset{1 \times L}{\boldsymbol{d}} \cdot \underset{L \times L}{\boldsymbol{F}} \tag{5.11}$$

where $\boldsymbol{F}$ represents the square matrix $L \times L$ of the Discrete Fourier Transform (DFT).

Since the transmitted signal in frequency-domain is $\boldsymbol{s} = [s_1, \ldots, s_L]$, the received signal for each antenna, $\boldsymbol{y}_1$ and $\boldsymbol{y}_2$, is given by equations

$$\underset{1 \times L}{\boldsymbol{y}_1} = \underset{1 \times L}{\boldsymbol{s}} \cdot \underset{L \times L}{\boldsymbol{H}_{11}} + \underset{1 \times L}{\boldsymbol{n}_1} \tag{5.12}$$

$$\underset{1 \times L}{\boldsymbol{y}_2} = \underset{1 \times L}{\boldsymbol{s}} \cdot \underset{L \times L}{\boldsymbol{H}_{12}} + \underset{1 \times L}{\boldsymbol{n}_2} \tag{5.13}$$

where $\boldsymbol{H}_{11}$ and $\boldsymbol{H}_{12}$ represent the channel's effect for transmitted channel 1 and channel 2. The same way, $\boldsymbol{n}_1$ and $\boldsymbol{n}_2$ represent the noise to respective channel.

After replacing equation 5.11 in equations 5.12 and 5.13, we can write

$$\underset{1 \times L}{\boldsymbol{y}_1} = \underset{1 \times L}{\boldsymbol{d}} \cdot \underset{L \times L}{\boldsymbol{F}.\boldsymbol{H}_{11}} + \underset{1 \times L}{\boldsymbol{n}_1} \tag{5.14}$$

$$\underset{1 \times L}{\boldsymbol{y}_2} = \underset{1 \times L}{\boldsymbol{d}} \cdot \underset{L \times L}{\boldsymbol{F}.\boldsymbol{H}_{12}} + \underset{1 \times L}{\boldsymbol{n}_2} \tag{5.15}$$

Thereby, the estimated signal from each receiving antenna, $\widehat{d}_1$ and $\widehat{d}_2$, is given by

$$\underbrace{\widehat{d}_1}_{1 \times L} = \underbrace{y_1}_{1 \times L} \cdot \underbrace{G_1 \cdot F^H}_{L \times L} \tag{5.16}$$

$$\underbrace{\widehat{d}_2}_{1 \times L} = \underbrace{y_2}_{1 \times L} \cdot \underbrace{G_2 \cdot F^H}_{L \times L} \tag{5.17}$$

where G and F^H represent the square matrix $L \times L$ of the equalizer coefficients and the inverse Discrete Fourier Transform coefficients (IDFT), respectively. Note that $F \cdot F^H = I_L$, where I_L represents the identity matrix of size $L \times L$.

Replacing equations 5.14 in 5.16 and 5.15 in 5.17, we can write

$$\underbrace{\widehat{d}_1}_{1 \times L} = \underbrace{d}_{1 \times L} \cdot \underbrace{F \cdot H_{11} \cdot G_1 \cdot F^H}_{L \times L} + \underbrace{n}_{1 \times L} \cdot \underbrace{G_1 \cdot F^H}_{L \times L} \tag{5.18}$$

$$\underbrace{\widehat{d}_2}_{1 \times L} = \underbrace{d}_{1 \times L} \cdot \underbrace{F \cdot H_{12} \cdot G_2 \cdot F^H}_{L \times L} + \underbrace{n}_{1 \times L} \cdot \underbrace{G_2 \cdot F^H}_{L \times L} \tag{5.19}$$

By analogy with the previous scheme, we can write

$$\widehat{d}_{1,j} = \underbrace{d_j \cdot f_j \cdot H_{11} \cdot G_1 \cdot f_j^H}_{Desired\ Signal} + \underbrace{\sum_{k=1,\ k \neq j}^{K} d_k \cdot f_k \cdot H_{11} \cdot G_1 \cdot f_j^H}_{ISI} + \underbrace{n_1 \cdot G_1 \cdot f_j^H}_{Noise} \tag{5.20}$$

$$\widehat{d}_{2,j} = \underbrace{d_j \cdot f_j \cdot H_{12} \cdot G_2 \cdot f_j^H}_{Desired\ Signal} + \underbrace{\sum_{k=1,\ k \neq j}^{K} d_k \cdot f_k \cdot H_{12} \cdot G_2 \cdot f_j^H}_{ISI} + \underbrace{n_2 \cdot G_2 \cdot f_j^H}_{Noise} \tag{5.21}$$

Since the MISO system, composed of a transmitting antenna and two receiving antennas (1×2), is equivalent to the sum of signals from two SISO systems with equivalents channels to H_{11} and H_{12}. Thereby, the estimated signal at the receiver is given by

$$\widehat{d}_j = \widehat{d}_{1,j} + \widehat{d}_{2,j} \tag{5.22}$$

$$\widehat{d}_j = \underbrace{d_j \cdot f_j \cdot (H_{11} \cdot G_1 + H_{12} \cdot G_2) \cdot f_j^H}_{Desired\ Signal} + \underbrace{\sum_{k=1,\ k \neq j}^{K} d_k \cdot f_k \cdot (H_{11} \cdot G_1 + H_{12} \cdot G_2) \cdot f_j^H}_{ISI}$$

$$+ \underbrace{n_1 \cdot G_1 \cdot f_j^H + n_2 \cdot G_2 \cdot f_j^H}_{Noise} \tag{5.23}$$

where f_j represents the j-th row of matrix F. Similar to the previous scheme, the data symbol vector is perfectly estimated at the receiver if $\sum_{k=1,\ k \neq j}^{K} d_k \cdot f_K \cdot (H_{11} \cdot G_1 + H_{12} \cdot G_2) \cdot f_j^H = 0$ and $n_1 \cdot G_1 \cdot f_j^H + n_2 \cdot G_2 \cdot f_j^H = 0$. Although these conditions not represent any real case, we can reduce more efficiently ISI and noise when compared to a for SISO system.

Table 5 shows the different equalizers used in this case. The equalization coefficients are defined as $g_{j,n}^{(i)}$, where i is the i-th transmit receive antenna, j is the j-th data symbol and n is the n-th subcarrier equalization as in SISO scheme and the equivalent channel is equal to $h = \left|h_{11,n}\right|^2 + \left|h_{12,n}\right|^2$.

Table 5 - Equalizers used in SIMO scheme

Maximum Ratio Combining	$g_{1,n}^{(i)} = h_{11,n}^*$ $g_{2,n}^{(i)} = h_{12,n}^*$
Equal Gain Combining	$g_{1,n}^{(i)} = \dfrac{h_{11,n}^*}{\left\|h_{11,n}\right\|}$ $g_{2,n}^{(i)} = \dfrac{h_{12,n}^*}{\left\|h_{12,n}\right\|}$
Zero Forcing Combining	$g_{1,n}^{(i)} = \dfrac{h_{11,n}^*}{\left\|h_{11,n}\right\|^2 + \left\|h_{12,n}\right\|^2}$ $g_{2,n}^{(i)} = \dfrac{h_{12,n}^*}{\left\|h_{11,n}\right\|^2 + \left\|h_{12,n}\right\|^2}$
Minimum Mean Square Error Combining	$g_{1,n}^{(i)} = \dfrac{h_{11,n}^*}{\left\|h_{11,n}\right\|^2 + \left\|h_{12,n}\right\|^2 + \sigma^2}$ $g_{2,n}^{(i)} = \dfrac{h_{12,n}^*}{\left\|h_{11,n}\right\|^2 + \left\|h_{12,n}\right\|^2 + \sigma^2}$

5.2.3. MIMO

In this case, we considered the simplest MIMO scheme with two antennas in both ends, as is shown in Figure 27. In the beginning, we start to analyze the signal received by one of the antennas, corresponding to a MISO system, because the received signal is the result of the sum of the signals received in both antennas.
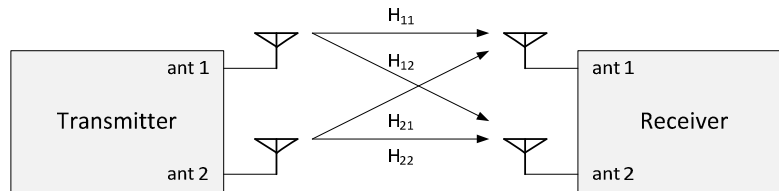

Figure 27 - MIMO scheme (2×2)

Assuming that we send L symbols, $\boldsymbol{d} = [d_1, \dots, d_L]$, the transmitted signal in the frequency-domain, $\boldsymbol{s}$, is given by

$$\underset{1 \times L}{\boldsymbol{s}} = \underset{1 \times L}{\boldsymbol{d}} \cdot \underset{L \times L}{\boldsymbol{F}} \tag{5.24}$$

where $\boldsymbol{F}$ represents the square matrix $L \times L$ of the Discrete Fourier Transform (DFT).

Since the transmitted signal in frequency domain is $\boldsymbol{s} = [s_1, \dots, s_L]$, we must bear in mind that the same symbols are sent by two different antennas. To perform the diversity gain introduced by MISO schemes was used Alamouti approach, see Table 6. In the first time slot, the transmit antennas 1 e 2 are sending symbols s_n and $-s_{n+1}^*$. In the next time slot are sent the symbols s_{n+1} and s_n^*, respectively.

Table 6 - Alamouti

	Transmitting antenna 1	Transmitting antenna 2
n	s_n	$-s_{n+1}^*$
n+1	s_{n+1}	s_n^*

Considering that the channels are constant over two adjacent subcarriers ($h_{1,n} = h_{1,n+1}$ and $h_{2,n} = h_{2,n+1}$), the received signal of two adjacent subcarriers, n and $n+1$, are given by

$$\boldsymbol{y} = \begin{cases} y_n = s_n.h_{1,n} - s^*_{n+1}.h_{2,n} + n_n \\ y_{n+1} = s_{n+1}.h^*_{1,n} + s^*_n.h^*_{2,n} + n_{n+1} \end{cases} \tag{5.25}$$

where $h_{1,n}$ and $h_{2,n}$ represent the channel's effect for transmitted channel 1 and channel 2. The same way, n_n and n_{n+1} represent the noise to respective channel.

Afterwards, the equalized signal for an arbitrary pair of adjacent subcarriers n and $n+1$, using the space frequency combining processing, is given by

$$\hat{\boldsymbol{r}} = \begin{cases} \hat{r}_n = y_n.g_{1,n} + y^*_{n+1}.g^*_{2,n} \\ \hat{r}_{n+1} = -y^*_n.g^*_{2,n}. + y_{n+1}.g_{1,n} \end{cases} \tag{5.26}$$

Replacing equations 5.25 in the equation 5.26, we can write

$$\hat{r}_n = s_n.h_{1,n}.g_{1,n} - s^*_{n+1}.h_{2,n}.g_{1,n} + n_n.g_{1,n}$$
$$+ s^*_{n+1}.h^*_{1,n}.g^*_{2,n} + d_n.h^*_{2,n}.g^*_{2,n} + n^*_{n+1}.g^*_{2,n} \tag{5.27}$$

After some mathematical manipulations, we can rewrite the previous equation

$$\hat{r}_n = \underbrace{s_n.\left(h_{1,n}.g_{1,n} + h^*_{2,n}.g^*_{2,n}\right)}_{Desired\ Symbol} + \underbrace{s^*_{n+1}.\left(h^*_{1,n}.g^*_{2,n} - h_{2,n}.g_{1,n}\right)}_{ICI}$$
$$+ \underbrace{\left(n_n.g_{1,n} + n^*_{n+1}.g^*_{2,n}\right)}_{Noise} \tag{5.28}$$

From equation 5.28 we can see that choosing the appropriate equalizer coefficients the inter carrier interference (ICI) is completely eliminated. Only using the EGC equalizer coefficients defined in Table 7 the term ICI is not fully removed.

After the IFFT operation, and using the same analogy of the other systems, the decision soft estimate of a generic data symbol j can be written as

$$\hat{d}_j = \underbrace{s_j.\boldsymbol{f}_j.\left(\boldsymbol{H}_1.\boldsymbol{G}_1 + \boldsymbol{H}^*_2.\boldsymbol{G}^*_2\right).\boldsymbol{f}^H_j}_{Desired\ Symbol}$$
$$+ \underbrace{\sum_{k=1,\ k \neq j}^{K} s_k.\boldsymbol{f}_k.\left(\boldsymbol{H}_1.\boldsymbol{G}_1 + \boldsymbol{H}^*_2.\boldsymbol{G}^*_2\right).\boldsymbol{f}^H_j}_{ISI} + Noise \tag{5.29}$$

As the received signal in the MIMO system is the sum of the received signal at each antenna, the expression that represents the equalized signal is equivalent to

$$\widehat{d}_j^{(2\times2)} = \widehat{d}_j^{(1)} + \widehat{d}_j^{(2)} \tag{5.30}$$

$$\widehat{d}_j^{(2\times2)} = \underbrace{d_j.f_j.(H_1.G_1 + H_2^*.G_2^* + H_3.G_3 + H_4^*.G_4^*).f_j^H}_{Desired\ Symbol}$$
$$+ \underbrace{\sum_{k=1,\ k\neq j}^{K} d_k^*.f_k^*.(H_1.G_1 + H_2^*.G_2^* + H_3.G_3 + H_4^*.G_4^*).f_j^H}_{ISI} + Noise \tag{5.31}$$

Table 7 shows the different equalizers used in this case. The equalization coefficients are defined as $g_{j,n}^{(i)}$, where i is the i-th transmit receive antenna, j is the j-th data symbol and n is the n-th subcarrier equalization as in SISO scheme and the equivalent channel is equal to $h = |h_{11,n}|^2 + |h_{12,n}|^2 + |h_{21,n}|^2 + |h_{22,n}|^2$.

Table 7 - Equalizers used in MIMO scheme

Maximum Ratio Combining	$g_{1,n}^{(i)} = h_{11,n}^*$
	$g_{2,n}^{(i)} = h_{21,n}^*$
	$g_{3,n}^{(i)} = h_{12,n}^*$
	$g_{4,n}^{(i)} = h_{22,n}^*$
Equal Gain Combining	$g_{1,n}^{(i)} = \dfrac{h_{11,n}^*}{|h_{11,n}|}$
	$g_{2,n}^{(i)} = \dfrac{h_{21,n}^*}{|h_{21,n}|}$
	$g_{3,n}^{(i)} = \dfrac{h_{3,n}^*}{|h_{12,n}|}$
	$g_{4,n}^{(i)} = \dfrac{h_{4,n}^*}{|h_{22,n}|}$

Zero Forcing Combining	$g_{1,n}^{(i)} = \dfrac{h_{11,n}^*}{\left\|h_{11,n}\right\|^2 + \left\|h_{21,n}\right\|^2 + \left\|h_{12,n}\right\|^2 + \left\|h_{22,n}\right\|^2}$ $g_{2,n}^{(i)} = \dfrac{h_{21,n}^*}{\left\|h_{11,n}\right\|^2 + \left\|h_{21,n}\right\|^2 + \left\|h_{12,n}\right\|^2 + \left\|h_{22,n}\right\|^2}$ $g_{3,n}^{(i)} = \dfrac{h_{12,n}^*}{\left\|h_{11,n}\right\|^2 + \left\|h_{21,n}\right\|^2 + \left\|h_{12,n}\right\|^2 + \left\|h_{22,n}\right\|^2}$ $g_{4,n}^{(i)} = \dfrac{h_{22,n}^*}{\left\|h_{11,n}\right\|^2 + \left\|h_{21,n}\right\|^2 + \left\|h_{12,n}\right\|^2 + \left\|h_{22,n}\right\|^2}$
Minimum Mean Square Error Combining	$g_{1,n}^{(i)} = \dfrac{h_{11,n}^*}{\left\|h_{11,n}\right\|^2 + \left\|h_{21,n}\right\|^2 + \left\|h_{12,n}\right\|^2 + \left\|h_{22,n}\right\|^2 + \sigma^2}$ $g_{2,n}^{(i)} = \dfrac{h_{21,n}^*}{\left\|h_{11,n}\right\|^2 + \left\|h_{21,n}\right\|^2 + \left\|h_{12,n}\right\|^2 + \left\|h_{22,n}\right\|^2 + \sigma^2}$ $g_{3,n}^{(i)} = \dfrac{h_{12,n}^*}{\left\|h_{11,n}\right\|^2 + \left\|h_{21,n}\right\|^2 + \left\|h_{12,n}\right\|^2 + \left\|h_{22,n}\right\|^2 + \sigma^2}$ $g_{4,n}^{(i)} = \dfrac{h_{22,n}^*}{\left\|h_{11,n}\right\|^2 + \left\|h_{21,n}\right\|^2 + \left\|h_{12,n}\right\|^2 + \left\|h_{22,n}\right\|^2 + \sigma^2}$

5.3. Numerical results

In this section, we present and discuss the main simulation results obtained for the discussed system. To evaluate the performance of the proposed MIMO SFBC SC-FDMA system with pre-processing mapping, we use the ITU pedestrian Rayleigh fading channel model B. We extended these time model to space-time, assuming that the distance between antenna elements is far apart to assume independent channels for each antenna, i.e., we assume independent fading processes at both sides. The channel is considered to be flat at least between two sub-carriers and is kept fixed over an OFDM symbol duration, but varies from OFDM to OFDM symbol. It is assumed that the receiver and transmitter have perfect knowledge of the channel. The channel coding scheme is the turbo-code defined in current LTE standard [4] with a coding rate of 1/3, combined with a puncturing process and an interleaver to have an overall coding rate of 3/2. The main system parameters are summarized in Table 8.

Table 8 - Main simulation parameters

Number of Carriers	1024 subcarriers
Number of Carriers per user	128 subcarriers
Frame Length	12 symbols
Total OFDM symbols duration	T_{OFDM} = 66.67 µs
Carrier Frequency	2GHz
Maximum Channel delay	2.47 µs
Number of paths	7
UT Velocity	10 Km/h
Modulation	QPSK
Number of users	1 user
Channel profile	ITU pedestrian channel model B
Modulation	QPSK

The configurable parameters used in the simulations are summarized in Table 9. Each simulation is a combination of these parameters performing all scenarios. The results are presented in terms of average bit error rate (BER) as function of E_b/N_0, i.e, the receiver energy per bit over the noise power spectral density without channel coding.

Table 9 - Configurable Parameters

Number of FFT tones	16 or 32 or 64 or 128
Channel coder	Off or CTC
Interleaver processing	On or Off
Equalizer's algorithms	MRC or EGC or ZFC or MMSEC
MIMO schemes	1×1 or 1×2 or 2×2

5.3.1. Schemes comparison without channel coding

The performance of the proposed scenarios is evaluated without channel coding. Figure 28, 29 and 30 show the performance results of the SFBC SC-FDMA approach for 1×1, 1×2 and 2×2 schemes with FFT size of 16 subcarriers and adjacent mapping, using MRC, EGC, ZFC and MMSEC equalizers.

We observe that the MMSEC outperforms the MRC, EGC, ZFC schemes, since the MMSEC can eliminate the ISI more efficiently. Nevertheless, ZFC has approximately the same performance than the MMSE for SIMO and MIMO cases. This performance is achieved without estimating the noise variance at the UT, contrary to the MMSEC, thus decreasing the UT complexity. On the

other hand ,we obtained a reduction of approximately 4 dB (for a BER target of 1.0e-3) of the ZFC against MMSEC in the SISO case. In conclusion, as we increase the spatial diversity (SISO to SIMO and SIMO to MIMO), MMSEC and ZFC converge to the same performance. EGC and MRC have much worse results when compared with the previous equalizers, since saturate too early, although EGC presents better results.

When comparing the various schemes of antennas, the increased spatial diversity improves the results. For instance, from SISO to SIMO case, we obtained a gain of approxiamtely 12 dB (for a BER target of 1.0e-3).

Also, we can observe that in MIMO case, the performance of the MRC pesents much better results than EGC because as it uses Alamouti, the EGC can not eliminate the interference between the two coded subcarriers, unlike the other equalizers including the MRC.
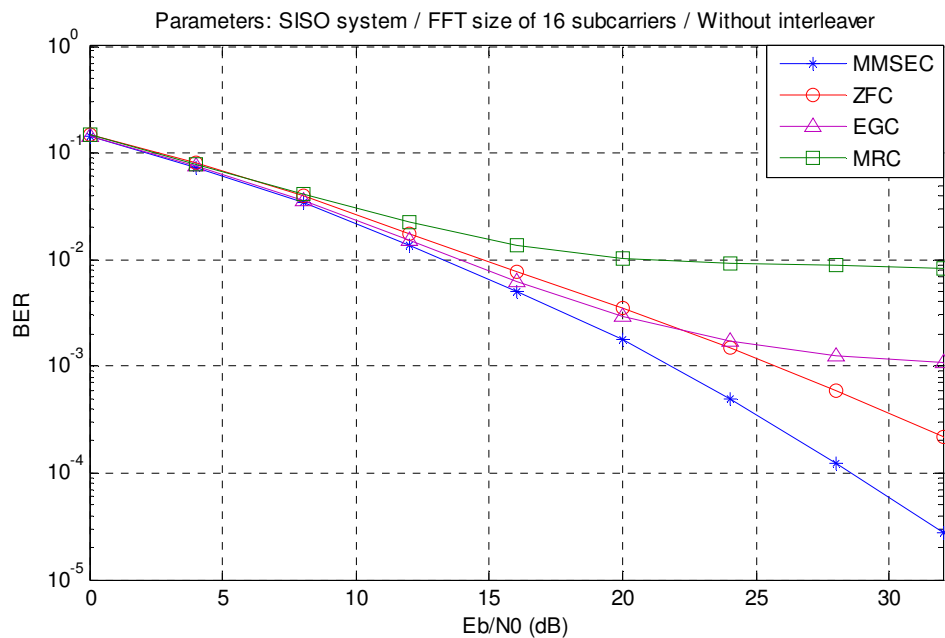
Figure 28 – Performance of equalization's algorithms without channel coding
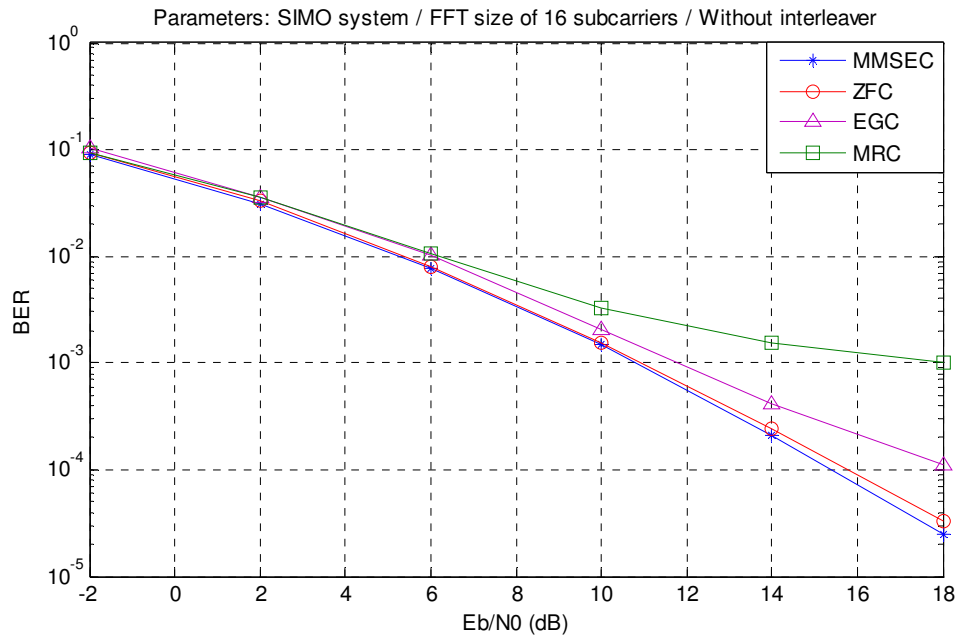
Figure 29 - Performance of equalization's algorithms without channel coding
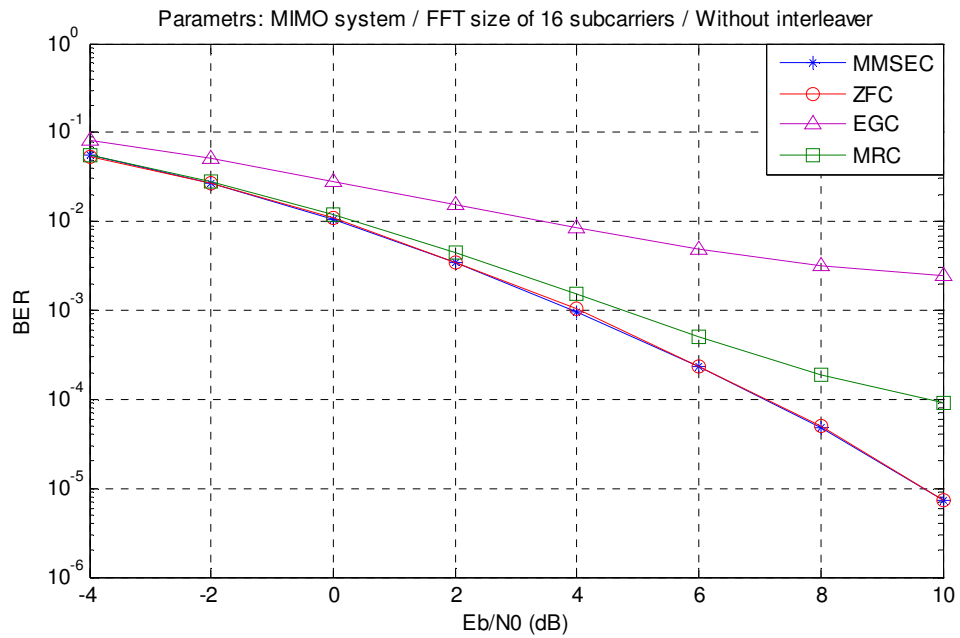
Figure 30 - Performance of equalization's algorithms without channel coding

Figure 31 and 32 show the performance results of the SFBC SC-FDMA approach for 1×1 and 1×2 schemes with FFT size of 16 subcarriers and interleaved mapping, using MRC, EGC, ZFC and MMSEC equalizers.

From these figures we can observe that the SISO and MIMO case have a similar behaviour with their counterparts with adjacent mapping, see Figures 28 and 29. However, that behavior is visible for lower values of E_b/N_0, for instance, we obtained a gain of approximately 8 dB (BER target of 1.0e-3) for SISO scheme and 4 dB (BER target of 1.0e-3) for SIMO scheme using MMSEC equalization. The reason behind this behavior is due to the decorrelation between the sub-channels that a given data symbol is transmitted, increasing thus the frequency diversity. When compared the same scenarios with different mapping mode, see Figures 28 and 30, ZFC has the same performance for SISO scheme, although it shows slight improvement in the BER curve for SIMO. Unlike the previously mentioned equalizers, we conclude that the uncorrelated carriers decrease the performance of MRC and EGC equalizer, because they cannot reduce efficiently the ISI.
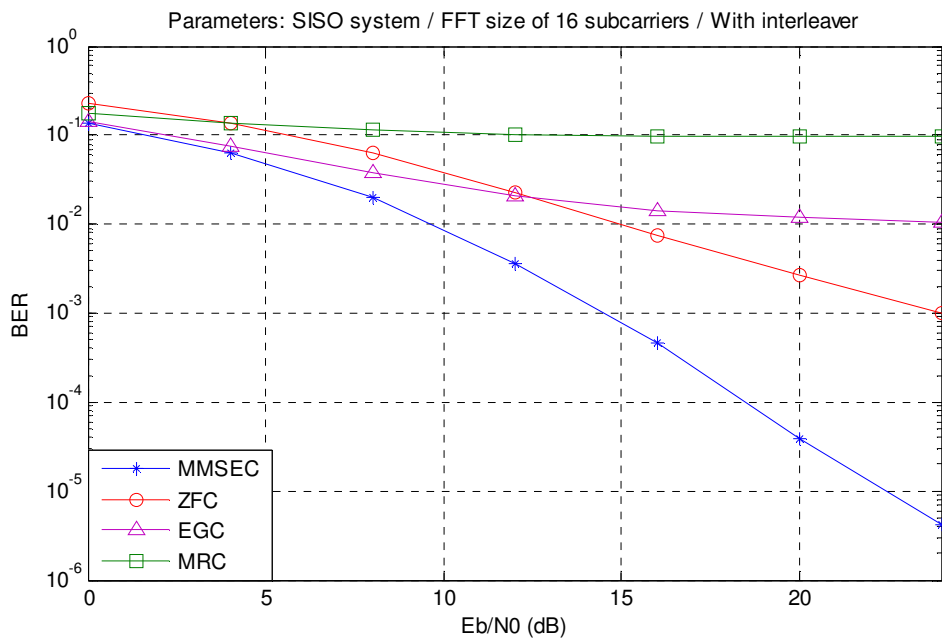
Figure 31 - Performance of equalization's algorithms without channel coding
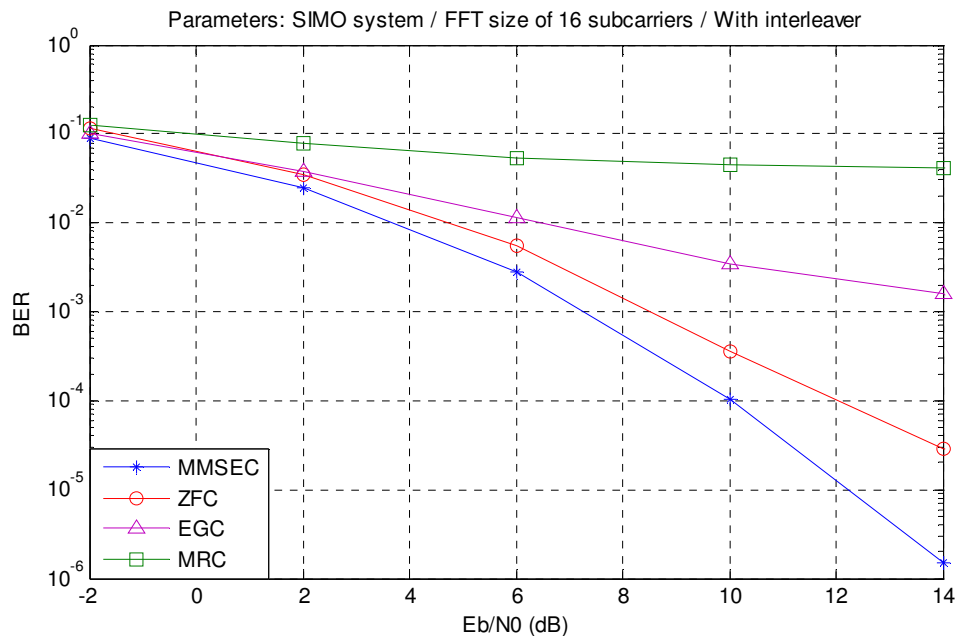
Figure 32 - Performance of equalization's algorithms without channel coding

Figures 33, 34 and 35 show the performance of the same schemes presented in previous Figures 28, 29 and 30, respectively, with the difference that the results were obtained using the referred FFT size of 128 subcarriers. From these figure we also can observe that the MMSEC outperform both ZFC, EGC and MRC, as well as increase the spatial diversity, the pair MRC and EGC and the pair ZFC and MMSEC converge to similar performance, separately.

Aditionally, the results are better for MMSEC when compared with the results for FFT size of 16 subcarriers because the frequency diversity is greater when we increase the number of carriers for each data symbol. Quantifying the gain introduced by the equalizer MMSEC, verifies that for a BER of 10e-3, the gain of this scenario compared to the same scenario with an FFT size of 16 subcarriers for SISO, SIMO and MIMO schemes is about 5 dB , 2 dB and 1 dB, respectively.

It was also found similar performance in both cases for ZFC, although the results are much worse for MRC and EGC.
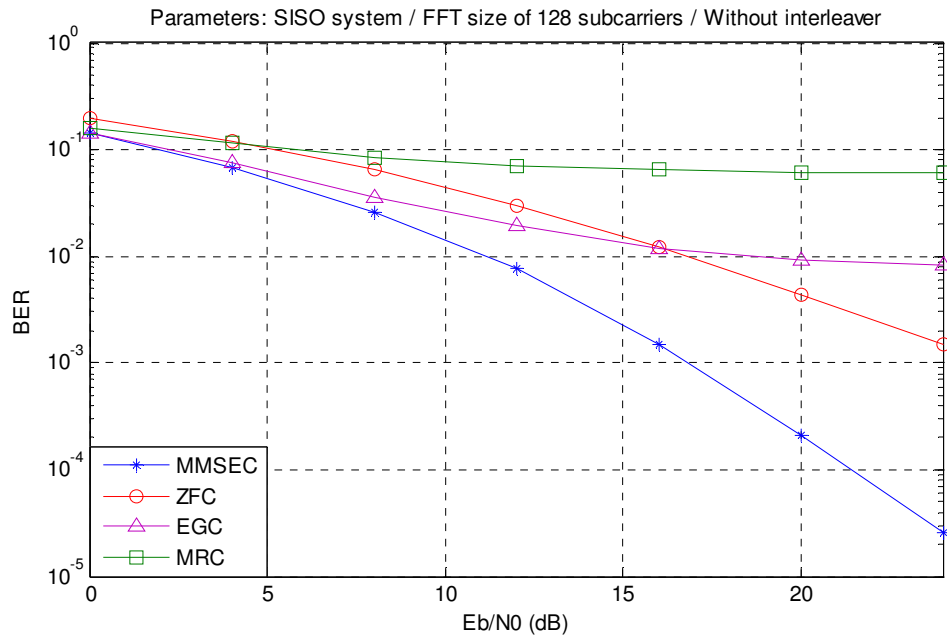
Figure 33 - Performance of equalization's algorithms without channel coding
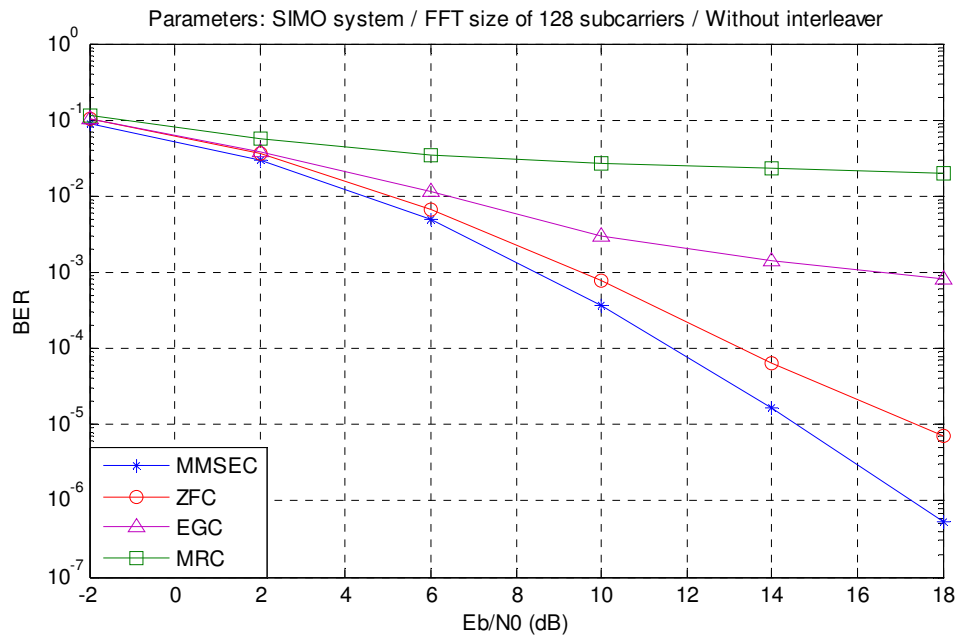
Figure 34 - Performance of equalization's algorithms without channel coding
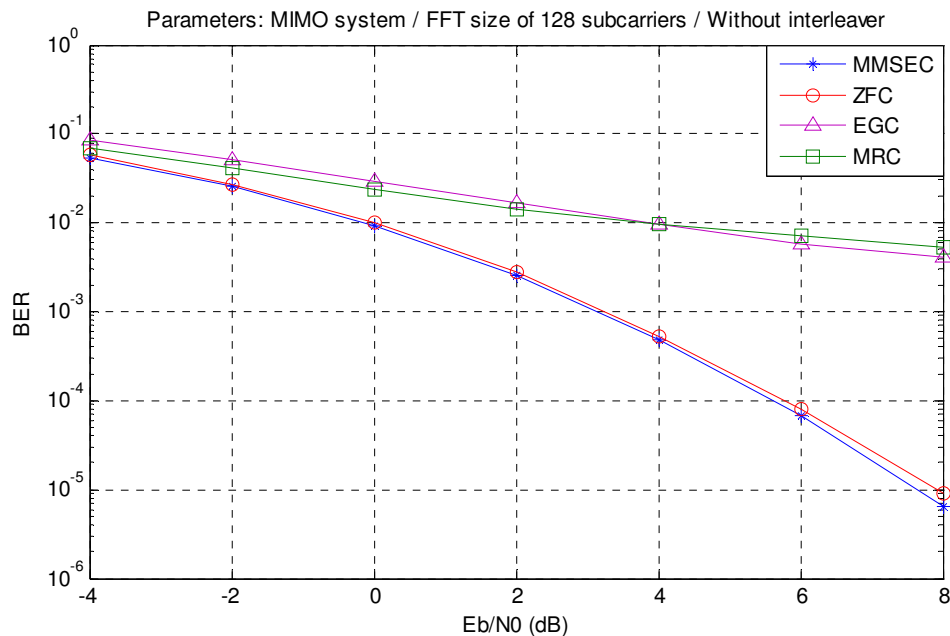
Figure 35 - Performance of equalization's algorithms without channel coding

Figures 36 and 37 show the performance of the same schemes presented in previous Figures 31 and 32, respectively, with the difference that the results were obtained using the referred FFT size of 128 subcarriers, as also can be compared with Figures 33 and 34, respectively, because the only difference is the mapping mode.

From these figures we can observe the same behavior of the Figures 31 and 32, but slightly more pronounced because the subcarriers are uncorrelated as possible. Thus, MRC and EGC have worse outcomes, in contrast, MMSEC and ZFC has more positive performance.

When compared with Figures 33 and 34, we obtained a gain of approximately 4 dB (BER target of 1.0e-3) for SISO scheme and 1.5 dB (BER target of 1.0e-3) for SIMO scheme using MMSEC equalization.
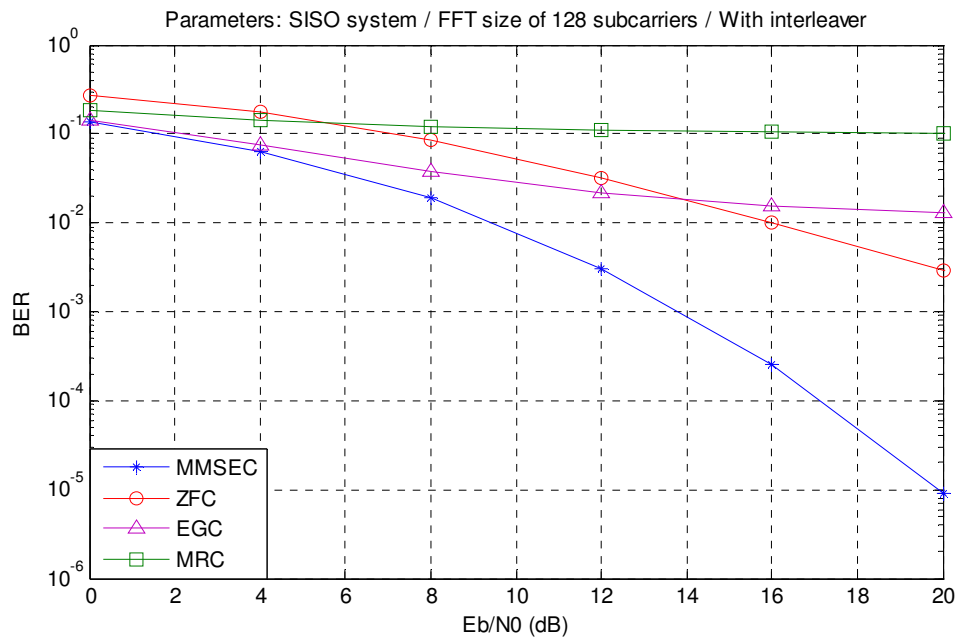
Figure 36 - Performance of equalization's algorithms without channel coding
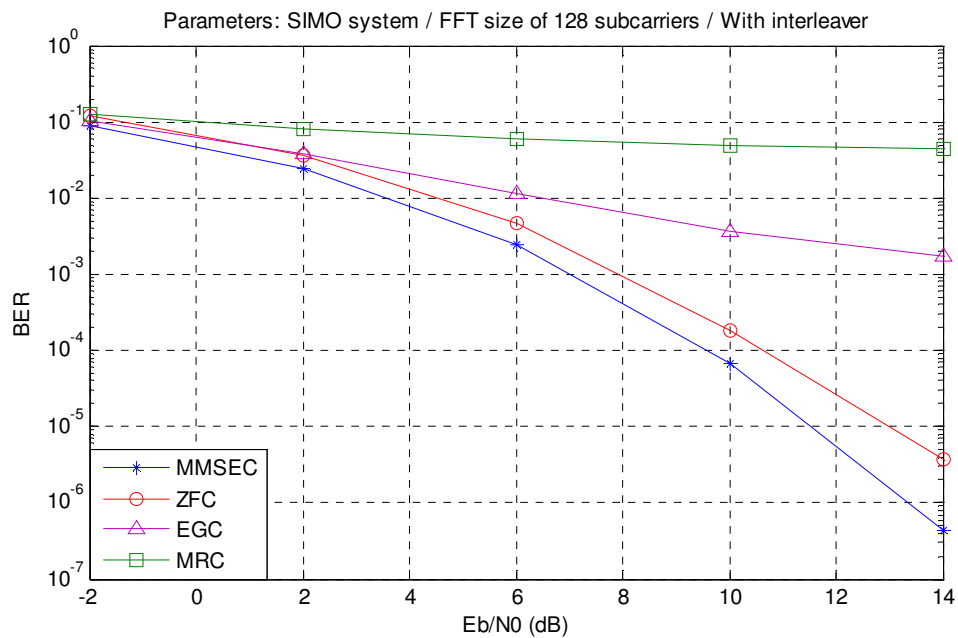
Figure 37 - Performance of equalization's algorithms without channel coding

5.3.2. Schemes comparison with channel coding

Then, the performance of the proposed scenarios is evaluated, considering typical pedestrian scenario and channel turbo coding based on LTE specifications, Convolutional Turbo Code (CTC).

Figure 38 and 39 show the performance results of the SFBC SC-FDMA approach for 1×1 and 1×2 schemes with FFT size of 16 subcarriers, adjacent mapping and channel codding, using MRC, EGC, ZFC and MMSEC equalizers.

As expected, the channel coding provides results far superior performance compared with the corresponding scenario without channel coding. However, in the SISO scheme we see that the ZFC equalizer presents the worst performance of all equalizers. This behavior is justified by the fact that beyond ZFC to mitigate ISI, will greatly amplify the noise.

Another interesting aspect can be seen in the MIMO case, as it uses Alamouti, the EGC can not eliminate the interference between the coded symbols, unlike the other equalizers including the MRC.
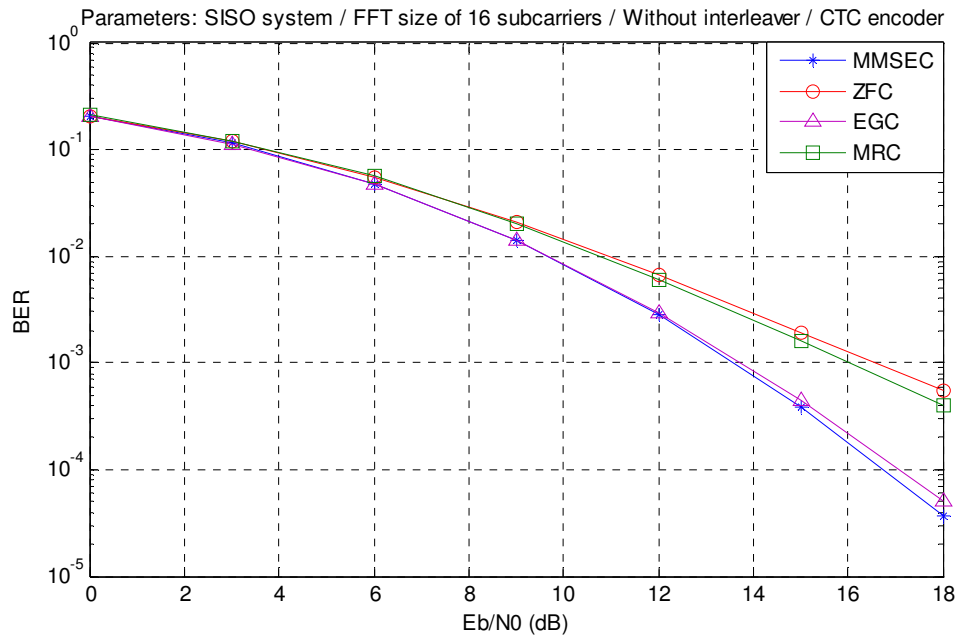

Figure 38 - Performance of equalization's algorithms with channel coding
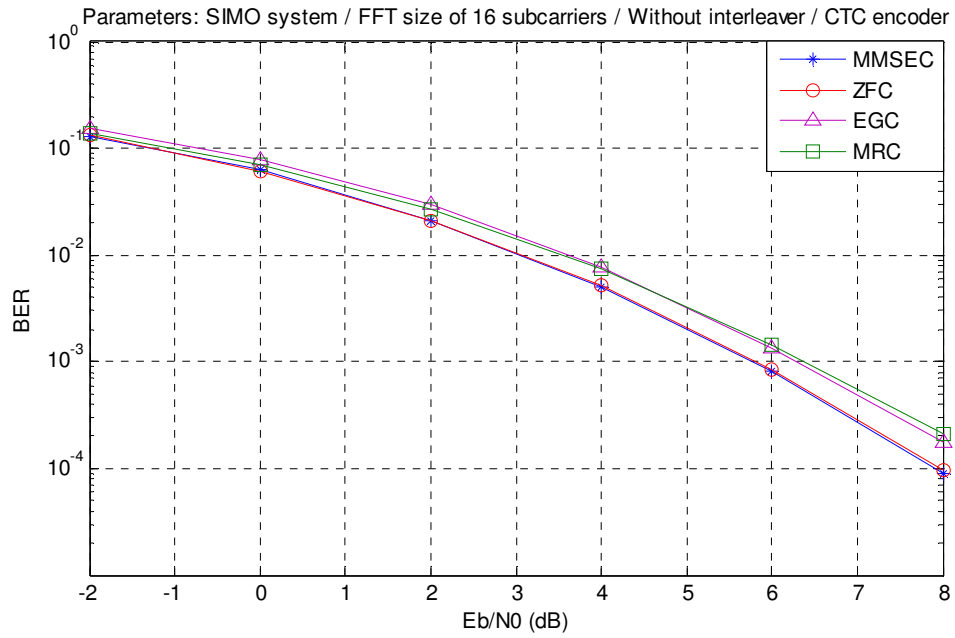
Figure 39 - Performance of equalization's algorithms with channel coding
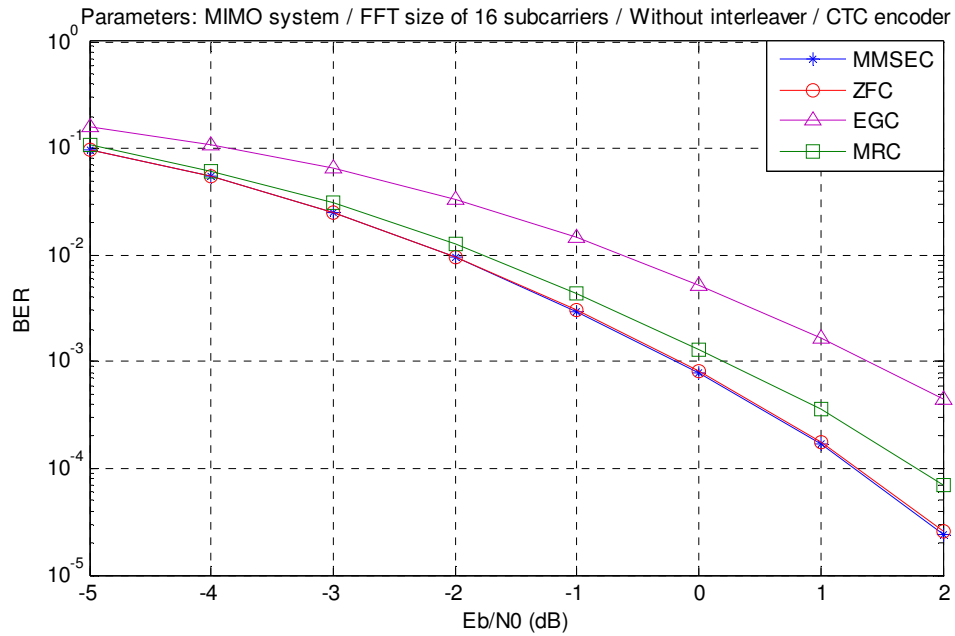
Figure 40 - Performance of equalization's algorithms with channel coding

In this case, Figure 41 and 42 show the performance results of the SFBC SC-FDMA approach for 1×1 and 1×2 schemes with FFT size of 16 subcarriers, interleaved mapping and channel codding, using MRC, EGC, ZFC and MMSEC equalizers.

There is a increase of efficient when we perform interleaved mapping, and once again, we observe that ZFC has poor performance when compared with others equalizers, presenting a serious disadvantage in real implementations because the schemes for the uplink antennas are most often in SISO and SIMO.

In the same scenario but without channel coding, we also observed a noticeable increase in efficiency, see Figures 31 and 32, the gain of this scenario for MMSE in SISO and SIMO schemes is about 5 dB and 2,5 dB, respectively, for a BER of 10e-3.
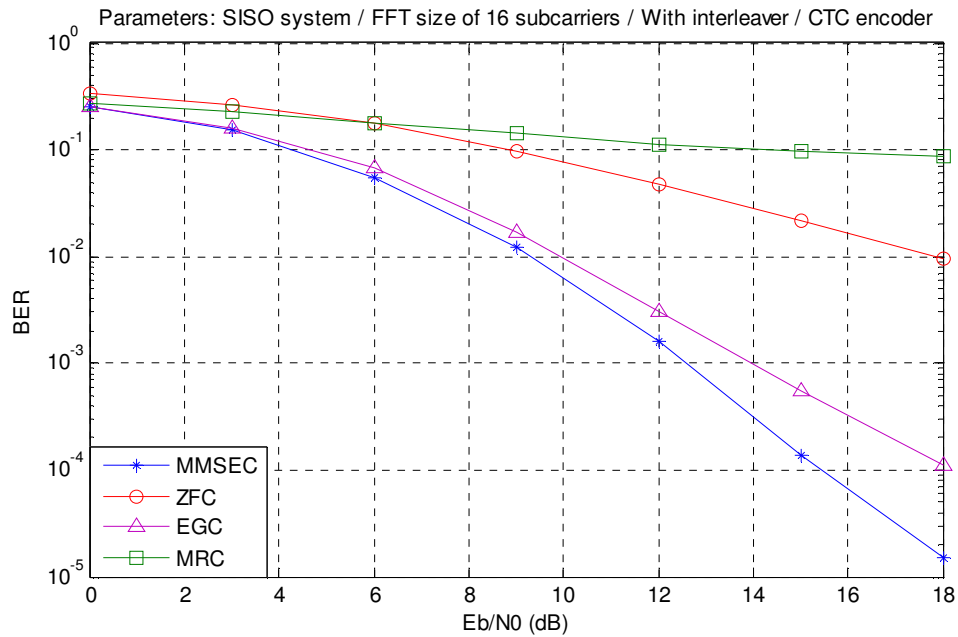

Figure 41 - Performance of equalization's algorithms with channel coding
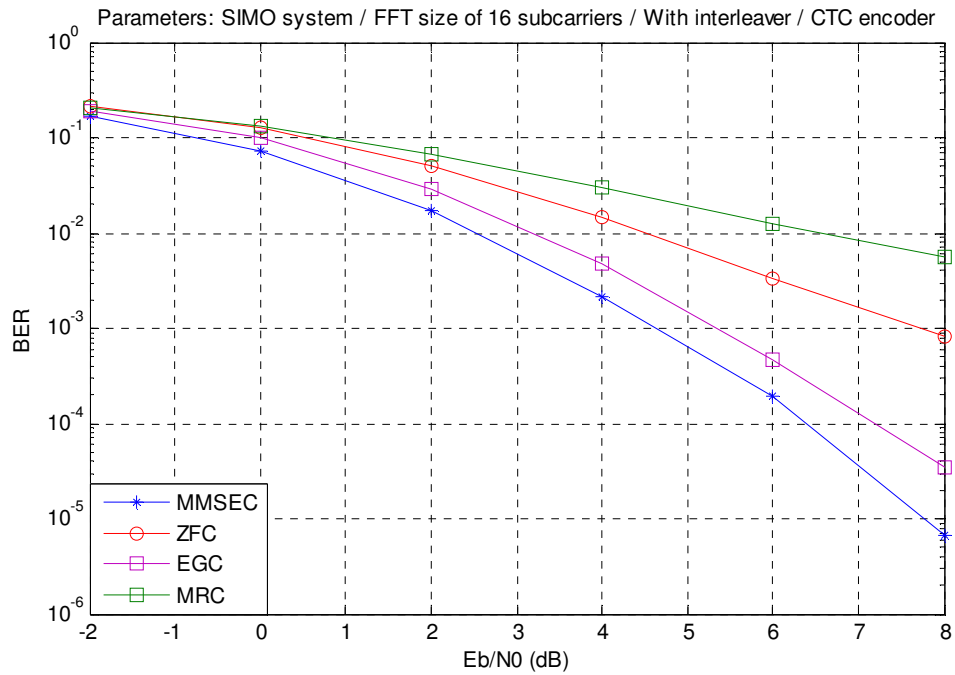
Figure 42 - Performance of equalization's algorithms with channel coding

Figure 43, 44 and 44 show the performance results of the SFBC SC-FDMA approach for 1×1, 1×2 and 2×2 schemes with FFT size of 128 subcarriers, adjacent mapping and channel codding, using MRC, EGC, ZFC and MMSEC equalizers.

Repeatedly, in the SISO and SIMO cases, the ZFC equalizer has lower performance in relation to the EGC due to reasons mentioned above, and for MIMO scheme, EGC behaves less efficient because uses Alamouti.

Despite all these considerations, we can not fail to mention that the scenario but with comparable FFT size of 16 subcarriers has better performance, i.e., the current setting for the equalizer MMSEC presents a reduction of approximately 2.8 dB, 1.2 dB and 0.7 dB even in cases SISO, SIMO and MIMO.
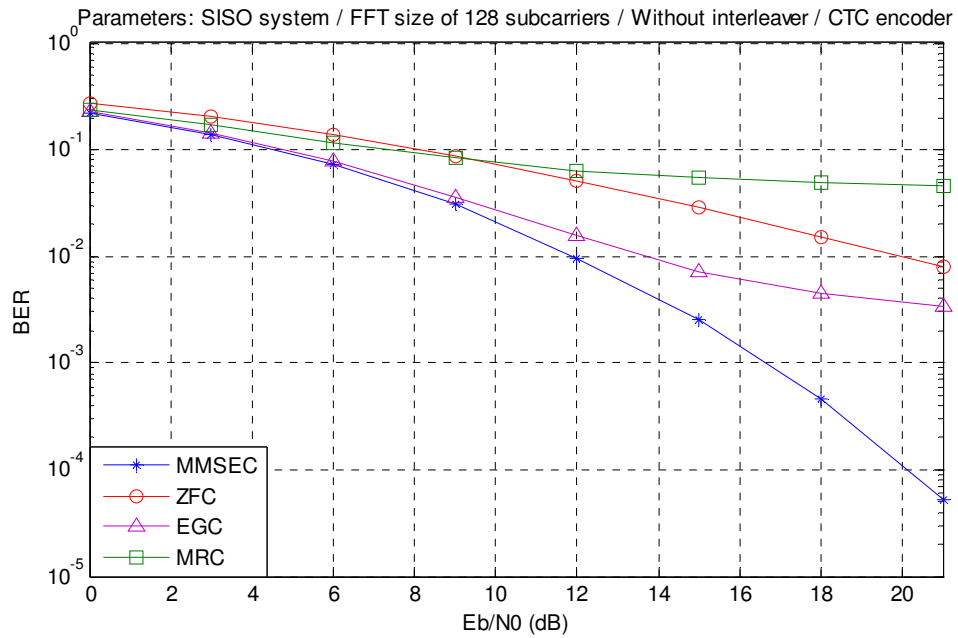
Figure 43 - Performance of equalization's algorithms with channel coding
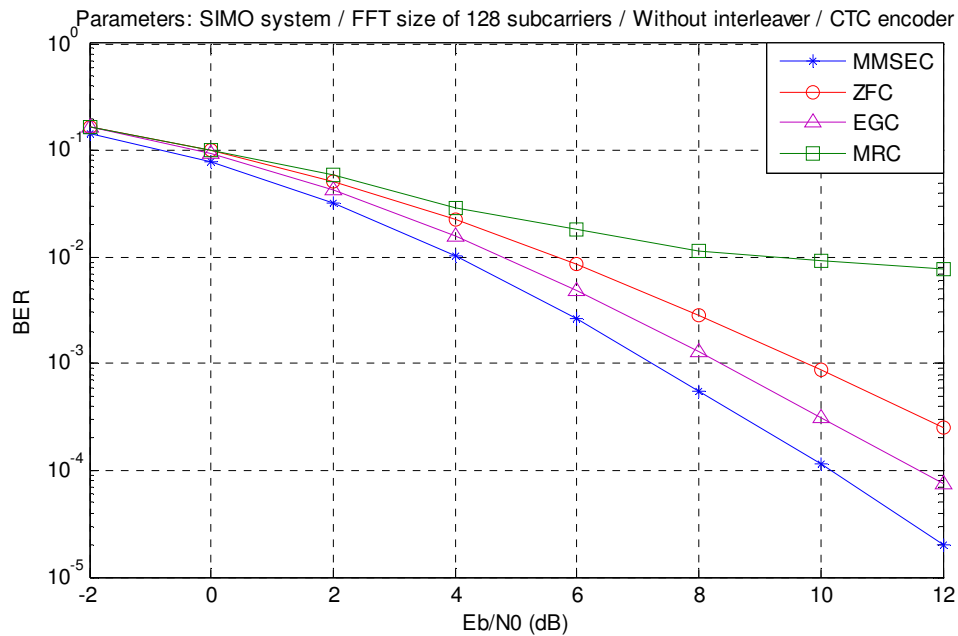
Figure 44 - Performance of equalization's algorithms with channel coding
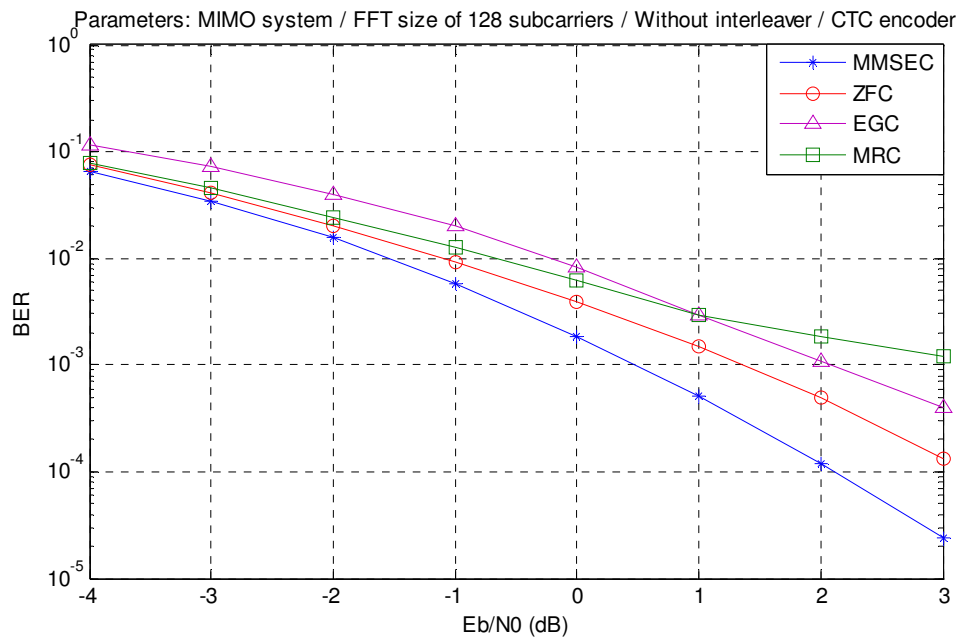
Figure 45 - Performance of equalization's algorithms with channel coding

Figure 46 and 47 show the performance results of the SFBC SC-FDMA approach for 1×1 and 1×2 schemes with FFT size of 128 subcarriers, interleaved mapping and channel codding, using MRC, EGC, ZFC and MMSEC equalizers.

In conclusion, these scenarios for SISO and SIMO schemes present the same behaviour than the equivalent scenario with FFT size of 16 subcarriers with a slightly lower performance.
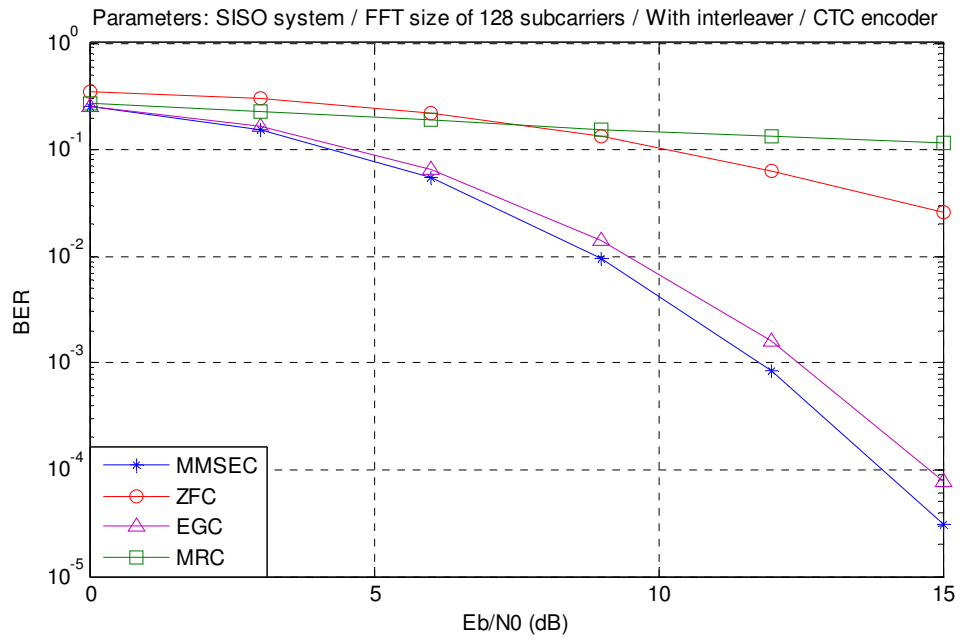
Figure 46 - Performance of equalization's algorithms with channel coding
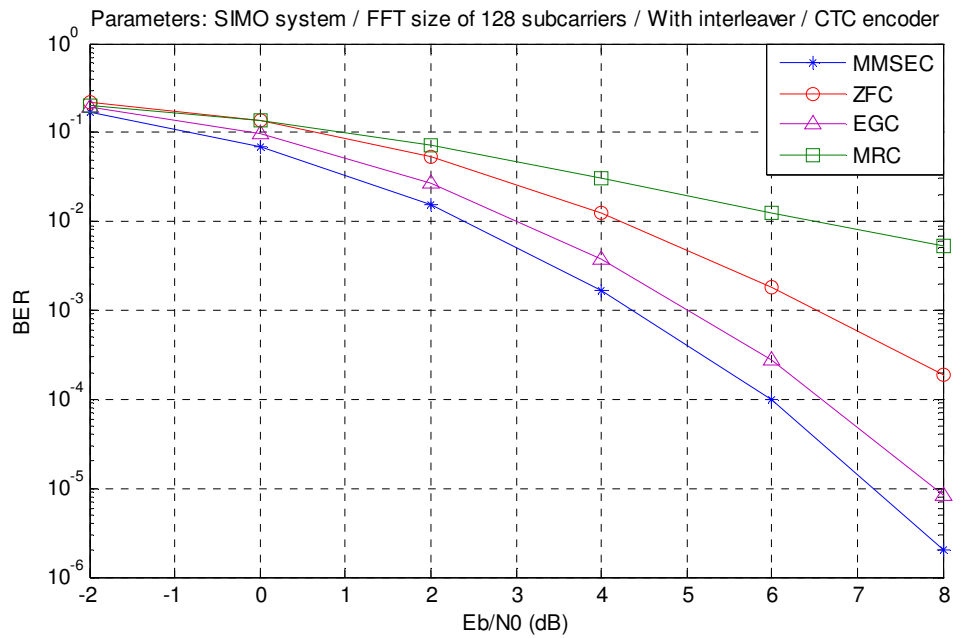
Figure 47 - Performance of equalization's algorithms with channel coding

Chapter 6

6. Conclusion

The wireless communication systems experienced major developments in the last three decades, marking each one a different generation. Since a simple communication via analog to the digital transmission with high transmission rates, long distance and fidelity, several new techniques and technologies have been implemented. This development was described in detail in Chapter 2 of this dissertation, presenting some concepts on the mobile communication systems as well as do an overview of the main features of LTE. In Chapter 2 we studied signal processing techniques specified in LTE, which help to achieve better results in terms of spectral efficiency of the system. The multicarrier techniques such as OFDM, allow to achieve high spectral gains. Other techniques such as OFDMA and SC-FDMA are also been described, since they are the key strategies in improving system performance. Then, in Chapter 3 was introduced the concept of multiple antennas in transmitter and receiver elements of the transmission. It has been shown that the use of systems that include multiple antennas will help achieve gains in these crucial systems, including the introduction of techniques for spatial diversity.

The goal of this practical work based on the simulation of wireless communications systems is analyze some strategies specified in LTE UL that improve the efficient of the transmission in terms of bit error rate. Thus, through the Simulink ™ tool of the Matlab ™ program were implemented chains of virtual SC-FDMA MIMO systems to several scenarios. In fact, the concept of spatial diversity and equalization are the basis of this study, so that the Chapter 5 was devoted to these issues. This chapter introduces the platform, and specifies the different techniques of spatial diversity (single input single output, single input multiple output and multiple input multiple output) and equalization (maximum ratio combining, equal gain combining, zero forcing combining and minimum mean square error combining) that were used in remaining work. It were created scenarios for the various antennas schemes where were simulated the various equalizers.

The analysis of results shows that the MMSEC equalizer is generally better than the ZFC, EGC and MRC. In the limit, ZFC presents the same performance than MMSEC for specific scenarios with large spatial diversity (1×2 and 2×2) and adjacent subcarriers highly correlated (with adjacent mapping and FFT size equal to 16 subcarriers). For these scenarios, the equalizer ZFC becomes advantageous because it is less complex and cheaper since they do not need to estimate the noise variance. Further, it was also observed that in general the MRC equalizer has the worst results in terms of bit error rate. However for very similar scenarios with high spatial diversity (2×2) and adjacent carriers highly correlated (with adjacent mapping and FFT size equal to 16 subcarriers),

MRC has better performance than EGC because as MIMO schemes uses Alamouti, the EGC can not eliminate the interference between symbols, unlike the other equalizers including the MRC.

Summarizing, the increased spatial diversity (1×1 to 1×2 and 1×2 to 2×2) and uncorrelated subcarriers carriers (interleaved mapping) allow to achieve significant improvements in critical mobile communication systems, especially for small values E_b/N_0.

As expected for scenarios with channel coding, we conclude that all results are significantly more efficient than its counterpart without channel coding. However, it is also observed that the equalizer ZFC has underperformed for the EGC or even the MRC. The reason behind this phenomenon is due to the amplification of noise by the ZFC equalizer when we consider the schemes 1×1 and 1×2. For 2×2 scheme with channel coding, EGC equalizer provide even lower results as previously stated.

Finally it was concluded that the use of spatial diversity and equalization techniques becomes quite useful when we want to use the spectrum more efficiently reaching higher data rates.

6.1. Future Work

In this thesis only single user/symbol equalizers were analyzed. It would be interesting simulate multi-user based equalizers to explicitly remove all the ISI, and compare the performance and complexity against the ones discussed in this work.

The results were obtained by assuming perfect knowledge of the channel at the base station. In practical systems the channel is estimated with errors, so it would be useful study how these errors impact on the system performance. For it is convenient to create a functional block with the function to estimate the effect of the various radio channels, similar to what happens in reality, as well as extend the spatial diversity systems for four antennas on both sides.

Bibliography

[1]   Farooq Khan, "LTE for 4G Mobile Broadband - Air Interface Technologies and Performance", Telecom R&D Center, Samsung Telecommunications, 2009.

[2]   Moray Rumney BSc, C. Eng, MIET, "3GPP LTE: Introducing Single-Carrier FDMA", in Issue 4 on Agilent Measurement Journal, 2008.

[3]   3GPP TS 36.211 V8.6.0, "Physical Channels and Modulation", Mar. 2009.

[4]   3GPP TS 36.212 V8.4.0, "Multiplexing and Channel Coding", Set. 2008.

[5]   3GPP website. [Online]. Available: http://www.3gpp.org

[6]   CDMA Development Group website. [Online]. Available: http://www.cdg.org

[7]   3GPP2 TSG C.S0024-0 v2.0, "cdma2000 High Rate Packet Data Air Interface Specification", Oct. 2000.

[8]   3GPP TR 25.848 v4.0.0, "Physical Layer Aspects of UTRA High Speed Downlink Packet Access", Mar. 2001.

[9]   3GPP2 TSG C.S0002-C v1.0, "Physical Layer Standard for cdma2000 Spread Spectrum Systems - Release C", May. 2002.

[10]   IEEE Std 802.16e-2005, "Air Interface for Fixed and Mobile Broadband Wireless Access Systems", 2005.

[11]   3GPP TR 25.912 v7.2.0, "Feasibility Study for Evolved Universal Terrestrial Radio Access (UTRA) and Universal Terrestrial Radio Access Network (UTRAN)", Aug. 2007.

[12]   3GPP2 TSG C.S0084-001-0 v2.0, "Physical Layer for Ultra Mobile Broadband (UMB) Air Interface Specification", Set. 2007.

[13]   3GPP TR 25.913 v7.3.0, "Requirements for Evolved Universal Terrestrial Radio Access (UTRA) and Universal Terrestrial Radio Access Network (UTRAN)", Mar. 2006.

[14]   3GPP TR 23.882 v1.15.1, "3GPP System Architecture Evolution: Report on Technical Options and Conclusions", Mar. 2008.

[15]   3GPP TR 36.913 v8.0.0, "Requirements for Further Advancements for E-UTRA (LTE-Advanced)", Jun. 2008.

[16] 4G Americas website. [Online]. Available: http://www.4gamericas.org

[17] Hannes Ekström, Anders Furuskär, Jonas Karlsson, Michael Meyer, Stefan Parkvall, Johan Torsner, and Mattias Wahlqvist, Ericsson, "Technical Solutions for the 3G Long-Term Evolution", IEEE Communications Magazine, Mar. 2006.

[18] White paper, "Transition to 4G: 3GPP Broadband Evolution to IMT-Advanced", Rysavy Research/3G Americas, Sep. 2010.

[19] White paper, "Coexistence of GSM-HSPA-LTE", 4G Americas, May 2011.

[20] 3GPP TS 36.104 V8.0.0, "Base Station (BS) Radio Transmission and Reception", Dec. 2007.

[21] Moray Rumney, "LTE and Evolution to 4G Wireless – Design and Measurement Challenges", Agilent Technologies, 2009.

[22] Stefania Sesia, Issam Toufik and Matthew Baker, "LTE – The UMTS Long Term Evolution", John Wiley & Sons, Ltd, 2009

[23] Harri Holma and Antti Toskala, "LTE for UMTS - OFDMA and SC-FDMA Based Radio Access", John Wiley & Sons, Ltd, 2009.

[24] Jim Zyren, "Overview of the 3GPP Long Term Evolution Physical Layer", Document Number: 3GPPEVOLUTIONWP REV 0, Freescale Semiconductor, 2007.

[25] 3GPP TS 36.101 V8.0.0, "User Equipment (UE) radio transmission and reception", Dec. 2007.

[26] Mr. Jacob Scheim, "SC-FDMA for 3GPP-LTE", Comsys Communication & Signal Processing Ltd, 2008.

[27] I. E. Telatar, "Capacity of Multi-Antenna Gaussian Channels", Lucent Technologies, Bell Laboratories.

[28] G. J. Foschini, and M. J. Gans, "On Limits of Wireless Communication in a Fading Environment when Using Multiple Antennas", Wireless Personal Communications, 1998.

[29] S. Yang, and F. Kaltenberger, "MIMO Algorithms for Wireless LAN", Proceedings Wireless Congress, Oct. 2005.

[30] D. Pérez Palomar, "A Unified Framework for Communications through MIMO Channels", Ph. D. Thesis, Universitat Politècnica de Catalunya, May 2003.

[31] S. M. Alamouti, "A Simple Transmit Diversity Technique for Wireless Communications", Bell Labs, Lucent Technologies

[32] A. van Zelst, R. van Nee, and G. A. Awater, "Space division multiplexing (SDM) for OFDM systems", Bell Labs, Lucent Technologies.

[33] V. Tarokh, N. Seshadri, and A. R. Calderbank, "Space-time codes for high data rate wireless communication: performance criterion and code construction", IEEE Transactions on Information Theory, Mar. 1998.

[34] Stefan Kaiser, "Space Frequency Block Coding and Code Division Multiplexing in ODFM Systems", IEEE Proceedings of GLOBECOM, 2003.